Age constraints for Paleoproterozoic glaciation in the Lake Superior Region: detrital zircon and hydrothermal xenotime ages for the Chocolay Group, Marquette Range Supergroup

Daniela A. Vallini, William F. Cannon, and Klaus J. Schulz

Abstract: A geochronological study of the Chocolay Group at the base of the Paleoproterozoic Marquette Range Supergroup in Michigan, Lake Superior Region, is attempted for the first time. Age data from detrital zircon grains and hydrothermal xenotime from the basal glaciogenic formation, the Enchantment Lake Formation, and the stratigraphically higher Sturgeon Quartzite and its equivalent, the Sunday Quartzite, provide maximum and minimum age constraints for the Chocolay Group. The youngest detrital zircon population in the Enchantment Lake Formation is 2317 ± 6 Ma; in the Sturgeon Quartzite, it is 2306 ± 9 Ma, and in the Sunday Quartzite, it is 2647 ± 5 Ma. The oldest hydrothermal xenotime age in the Enchantment Lake Formation is 2133 ± 11 Ma; in the Sturgeon Quartzite, it is 2115 ± 5 Ma, and in the Sunday Quartzite, it is 2207 ± 5 Ma. The radiometric age data in this study implies the depositional age of the Chocolay Group is constrained to ~2.3–2.2 Ga, which proves its correlation with part of the Huronian Supergroup in the Lake Huron Region, Ontario, and reveals the unconformity that separates the Chocolay Group from the overlying Menominee Group is up to 325 million years in duration. The source(s) of the ~ 2.3 Ga detrital zircon populations in the Enchantment Lake Formation and Sturgeon Quartzite remains an enigma because no known rock units of this age are known in the Michigan area. It is speculated that once widespread volcano-sedimentary cover sequences in Michigan were removed or concealed prior to Chocolay Group deposition. The hydrothermal xenotime ages probably reflect basinal hydrothermal fluid flow associated with the period of extension, involving rifting and major dyke formation, that affected the North American provinces between 2.2 and 2.1 Ga.

Résumé : Une étude géochronologique du Groupe de Chocolay, à la base du Supergroupe de Marquette Range (Paléoprotérozoïque), au Michigan, dans la région du lac Supérieur, est effectuée pour la première fois. Des données sur les âges à partir de grains détritiques de zircon et de xénotime provenant de la formation glaciogénique basale, de la Formation de Enchantment Lake et du quartzite de Sturgeon à position stratigraphique plus élevée, ainsi que de son équivalent, le quartzite Sunday, fournissent les âges limites maximum et minimum pour le Groupe de Chocolay. La population de zircons détritiques les plus jeunes date de 2317 ± 6 Ma dans la Formation de Enchantment Lake, de 2306 ± 9 Ma dans le quartzite de Sturgeon et de 2647 ± 5 dans le quartzite de Sunday. Le plus vieil âge pour un xénotime hydrothermal est de 2133 ± 11 Ma dans la Formation de Enchantment Lake, de 2115 ± 5 Ma dans le quartzite de Sturgeon et de 2207 ± 5 Ma dans le quartzite de Sunday. Les données d'âge radiométrique dans la présente étude limitent l'âge de déposition du Groupe de Chocolay à ~2,3–2,2 Ga, ce qui prouve sa corrélation avec une partie du Supergroupe de l'Huronien dans la région du lac Huron, en Ontario, et révèle que la discordance qui sépare le Groupe de Chocolay du Groupe de Menominee sus-jacent a possiblement duré jusqu'à 325 Ma. La ou les sources des populations de zircon détritique, ~2,3 Ga, dans la Formation de Enchantment Lake et dans le quartzite de Sturgeon demeure une énigme car aucune unité rocheuse de cet âge n'est connue dans la région de Michigan. L'hypothèse est posée qu'il y a déjà eu des séquences volcano-sédimentaires étendues au Michigan qui auraient été enlevées ou dissimulées avant la déposition du Groupe de Chocolay. Les âges du xénotime hydrothermal sont probablement le reflet d'un écoulement de fluides hydrothermaux de base associé à la période d'extension, avec la formation de rifts et de dykes majeurs, qui a touché les provinces nord-américaines il y a 2,2–2,1 Ga.

[Traduit par la Rédaction]

Received 12 April 2005. Accepted 30 January 2006. Published on the NRC Research Press Web site at http://cjes.nrc.ca on 1 June 2006.

Paper handled by Associate Editor W. Davis.

D.A. Vallini.[1] School of Earth and Geographical Sciences, University of Western Australia, 35 Stirling Highway, Crawley, WA 6009, Australia.
W.F. Cannon and K.J. Schulz. US Geological Survey, 954 National Center, Reston, VA 20192, USA.

[1]Corresponding author (e-mail: daniela.vallini@woodside.com.au).

 doi:10.1139/E06-010

Introduction

Correlation of the Marquette Range Supergroup in Michigan and Wisconsin, USA, with the Huronian Supergroup in Ontario, Canada, has been a subject of interest and debate for many years. These thick Paleoproterozoic sedimentary successions play an important role in the understanding of the evolution of North America and, in particular, Paleoproterozoic glacial episodes. Until recently, there has been little age data for the Marquette Range Supergroup; its correlation with the Huronian Supergroup has been largely based on lithologic and stratigraphic similarities and the broad age constraints provided by the ages of basement rocks and rocks that intrude these successions. The Huronian Supergroup, which can be as thick as 12 km, lies unconformably on Archean basement and contains three diamictite and dropstone-bearing formations: the Ramsey Lake, the Bruce, and the Gowganda formations. Correlation of the basal glaciogenic units of the Marquette Range Supergroup, with the Gowganda Formation exposed ~200 km to the east in Ontario, was proposed by Young (1973, 1983), Gair (1981), and Ojakangas (1982, 1985). Only one glaciogenic horizon is present in Michigan, and it has been correlated with the uppermost glaciogenic unit in the Huronian sequence (e.g., Ojakangas 1982; Young 1983); however, it is possible that other glaciogenic units in Michigan were removed by erosion (Ojakangas et al. 2001). The glacial units in the Huronian Supergroup have also been correlated with similar deposits in the Snowy Pass Group, Wyoming (Young 1970, 1973; Graff 1979; Houston et al. 1981), in the Chibougamau Formation, Quebec, and in the Padlei Formation, Northwest Territories (Long 1981; Young and McLennan 1981). The ages of the North American glaciogenic units are not tightly constrained; the best constraints are those of the Huronian Supergroup. The lower part of the Huronian sequence, the Elliot Lake Group, consists of a volcanic sequence which interfingers with, and is overlain by, metasedimentary rocks. In the Sudbury area (Fig. 1), the volcanic sequence is known as the Copper Cliff Formation and contains a rhyolite dated at 2450 ± 25 Ma (U–Pb zircon, Krogh et al. 1984). Layered gabbro anorthosite intrusions were emplaced into Archean crust at the base of the Huronian supracrustal sequences in some areas such as Sudbury, and several have been dated at 2491 ± 5 and 2480 ± 10 Ma (U–Pb zircon, Krogh et al. 1984). The lower part of the Elliot Lake Group is locally intruded by the Murray and Creighton granites. The Murray granite has a U–Pb zircon age of 2477 ± 9 Ma (Krogh et al. 1996), and the Creighton granite is made up of two phases, one with an age of 2414 ± 5 Ma and the other of 2377 ± 2 Ma (Smith 2002). The Nipissing diabase, a collection of tholeiitic gabbro sills and dykes, crosscuts the entire Huronian sequence (Van Schmus 1965; Fairbairn et al. 1969) and has a U–Pb baddeleyite age of 2219 ± 4 Ma (Corfu and Andrews 1986). These ages imply that, if the proposed correlation between the Marquette Range Supergroup and Huronian Supergroup is correct, the base of the Marquette Range Supergroup was deposited between ~2.5 and 2.2 Ga. Without this correlation, the lower Marquette Range Supergroup is constrained between ≥2.6 Ga, the age of the underlying Archean basement rocks, and 1874 ± 9 Ma, the age of a rhyolite (U–Pb zircon, Schneider et al. 2002) from the Hemlock Formation in the Menominee Group (Fig. 2).

We report here U–Pb geochronological data for detrital zircon grains from several formations of the Chocolay Group; these data give maximum depositional ages and provide insight into sediment provenance areas. From the same formations, we also report ages of hydrothermal xenotime (YPO_4) crystals which have apparently formed in situ and thus provide a minimum age for sedimentation. Xenotime can form during diagenesis of siliciclastic sediments (e.g., McNaughton et al. 1999; Fletcher et al. 2000; Vallini et al. 2002, 2005, in press; Rasmussen et al. 2004) and during episodes of metamorphism or hydrothermal fluid flow (e.g., Rasmussen et al. 2001, 2002; Rasmussen and Fletcher 2002; Dawson et al. 2003; Kositcin et al. 2003; Vielreicher et al. 2003). Careful petrography, in combination with geochronology, is required to resolve the origin of individual xenotime crystals. Several recent studies of the mineral, utilizing the sensitive high-resolution ion microprobe (SHRIMP) in situ analysis, have provided U–Pb age constraints for sedimentation (e.g., McNaughton et al. 1999; Fletcher et al. 2000; Vallini et al. 2002, 2005, in press; Rasmussen et al. 2004).

Geological setting

During the Paleoproterozoic, the Lake Superior Region was the site of deposition of a thick volcano-sedimentary succession onto the Archean (3.5–2.6 Ga) greenstone–granite and gneiss terranes (Fig. 1) of the southern margin of the Superior craton. This succession is known as the Marquette Range Supergroup (Cannon and Gair 1970) in Michigan and Wisconsin and as the Mille Lacs, North Range, and Animikie groups in east-central Minnesota and adjoining Ontario. The principal stratigraphic terminology for the Marquette Range Supergroup was originally defined by James (1958) and has been little changed since. James (1958) defined three groups consisting of the basal Chocolay Group overlain successively by the Menominee and Baraga groups, each group being bounded by disconformities or low-angle unconformities (Fig. 2). A fourth group, the Paint River Group, was believed by James (1958) to be the youngest of the four, although structural complications make this correlation uncertain.

The Chocolay Group (Fig. 2), the focus of this study, is a succession of glaciogenic rocks, quartzite, and dolomite. Rocks of this group are only sporadically preserved beneath a regional unconformity at the base of the Menominee Group, with remnants in the eastern Marquette Range and nearby Dead River Basin, parts of the Menominee Range, and the Gogebic Range (Fig. 3). There are no recorded Chocolay equivalents in east-central Minnesota and adjoining Ontario (Fig. 1) owing to either non-deposition or erosion prior to deposition of the Animikie Group. The basal glaciogenic deposits of the Chocolay Group are only found in three areas in northern Michigan: the Fern Creek Formation (~80 m thick) in the Menominee Range, the Enchantment Lake Formation (~150 m thick) in the eastern Marquette Range, and the Reany Creek Formation (~1 km thick) in the Dead River Basin (Fig. 3). In the eastern Gogebic Range, a thin (<10 m) boulder bed underlies the Chocolay Group quartzites (Allen and Barrett 1915). One of the most compre-

Fig. 1. Generalized distribution of Archean and Paleoproterozoic rocks in the Great Lakes Region (modified from Young 1983). Labelled features in the region are discussed in the text. The box outlines the area in Fig. 3.

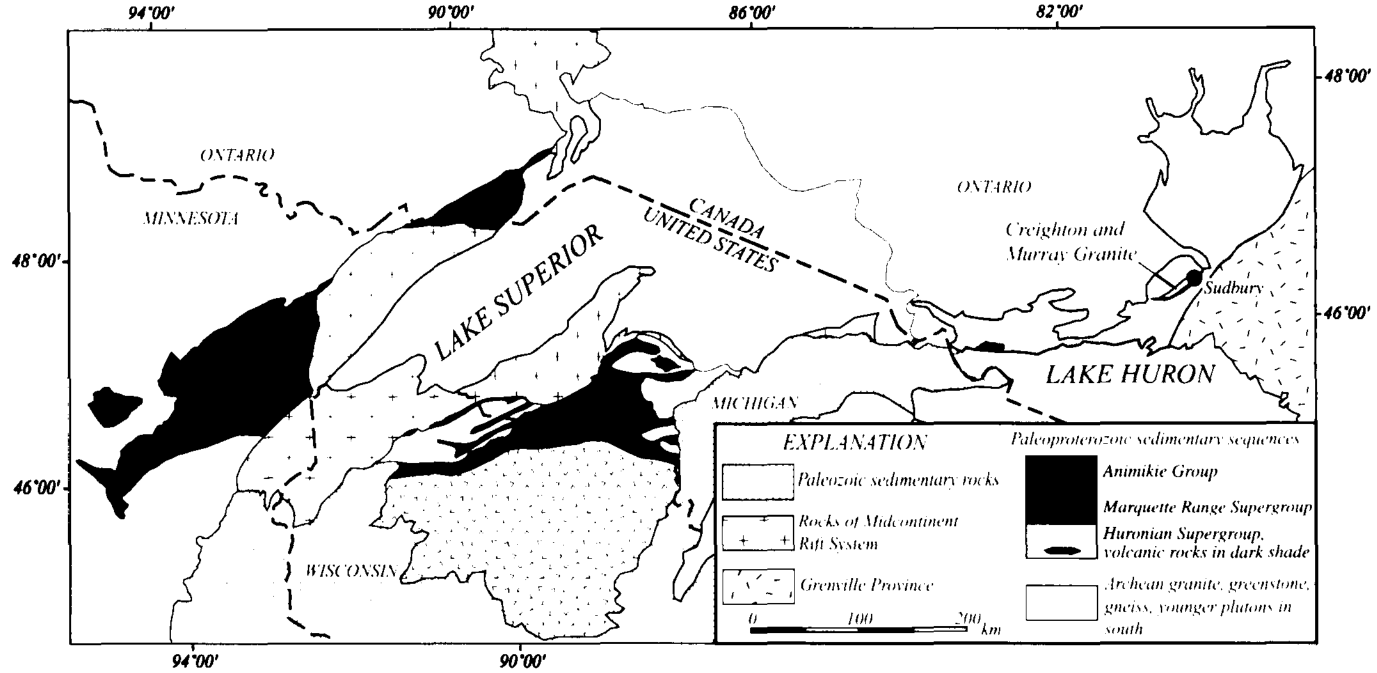

hensive descriptions of the Enchantment Lake Formation is given by Gair (1975). The three glaciogenic formations in Michigan are considered correlative by Gair and Thaden (1968), Young (1973, 1983), and Ojakangas (1982, 1985). Diamictites (Pettijohn 1943; Puffett 1969; Young 1973; Gair 1981) and dropstone units (Ojakangas 1982) have been observed at each of the three areas in Michigan. Low chemical index of alteration values, consistent with a glacial origin, were recorded in the unweathered parts of the basal glaciogenic deposits of the Chocolay Group (Argast 2002). Although the glaciogenic origin of these rocks has been questioned by some investigators (e.g., Larue 1981), the stratigraphic juxtaposition and interlayering of diamictites with dropstone units suggests deposition in either a nonmarine glacially influenced environment or a glacially influenced continental margin (Ojakangas 1988).

There is an unconformity of uncertain duration between the glacial diamictite deposits and the overlying quartzites. The top of the glacial formation is locally marked by the possible remnants of a paleosol (Ojakangas et al. 2001). However, there is still some debate as to the nature of this contact because the Enchantment Lake Formation in the Marquette Range appears to grade upward into the overlying quartzite formation (e.g., Gair 1981).

The overlying quartzite formation is variously known as the Mesnard Quartzite in the eastern Marquette Range, the Sunday Quartzite in the eastern Gogebic Range, and the Sturgeon Quartzite in the Menominee Range (Figs. 1–3). These quartzites are sericite-rich near the base of the formation and grade upward into mineralogically mature (95% quartz) quartzite. It was thought by Ojakangas et al. (2001) that they may be the products of erosion and reworking of deeply weathered source rocks that were then deposited over a wide area during a marine transgression onto a continental margin. In some places, such as in the Marquette Range, the quartzites are thicker along present day structural troughs and display paleocurrent directions parallel to trough axes, which suggests that there may have been precursor structures that were active during sedimentation (Larue and Sloss 1980; Larue 1981). Elsewhere, the quartzites appear to be blanket sands deposited on a stable platform (Larue 1981). These platformal quartzites (e.g., in the Gogebic Range) give polymodal paleocurrent directions (Larue 1981).

The quartzite units grade upward into thick beds of dolomite that contain structures implying formation during warm arid conditions (Taylor 1972; Larue 1981). The dolomite strata are topped by an unconformity everywhere except in the eastern part of the Marquette Range, where the dolomite is overlain by a thin unit of mudstone of terrigenous and possibly partly volcanic derivation (Gair 1975). The contact between the Chocolay and younger groups is a disconformity when viewed on a local scale with no discernible angular discordance. Only at a more regional scale, does the Menominee Group transect and truncate the Chocolay Group. Metamorphic grade of the Chocolay Group in the Menominee Range ranges from chlorite to biotite grade (James 1955; Bayley et al. 1966; Larue 1981), and that in the eastern Marquette Range and eastern Gogebic Range is chlorite grade.

The Superior craton was originally part of the Kenorland supercontinent (Williams et al. 1991), which amalgamated at ~ 2.8–2.6 Ga, and comprised the Archean provinces of the North America, Fennoscandian (Baltic), and Siberian shields (Young 1991; Hoffman 1992; Aspler and Chiarenzelli 1998; Ojakangas et al. 2001). The Kenorland supercontinent started rifting at ~2.45 Ga in Ontario, with initial rifting represented by basal mafic volcanic rocks in the Huronian Supergroup (e.g., Heaman 1997; Ojakangas et al. 2001). Final breakup was marked by a host of 2.2–2.1 Ga mafic dyke and sill

Fig. 2. Generalized stratigraphic column of the Marquette Range Supergroup in Michigan and Wisconsin and the Huronian Supergroup in Ontario. Only formations mentioned in the text are labelled in this illustration. Straight lines are conformable contacts and wavy lines represent unconformities. Not to scale. Age references are (1) Schneider et al. (2002), (2) Corfu and Andrews (1986), (3) Krogh et al. (1996), (4) Smith (2002), (5) Krogh et al. (1984). Fm, Formation.

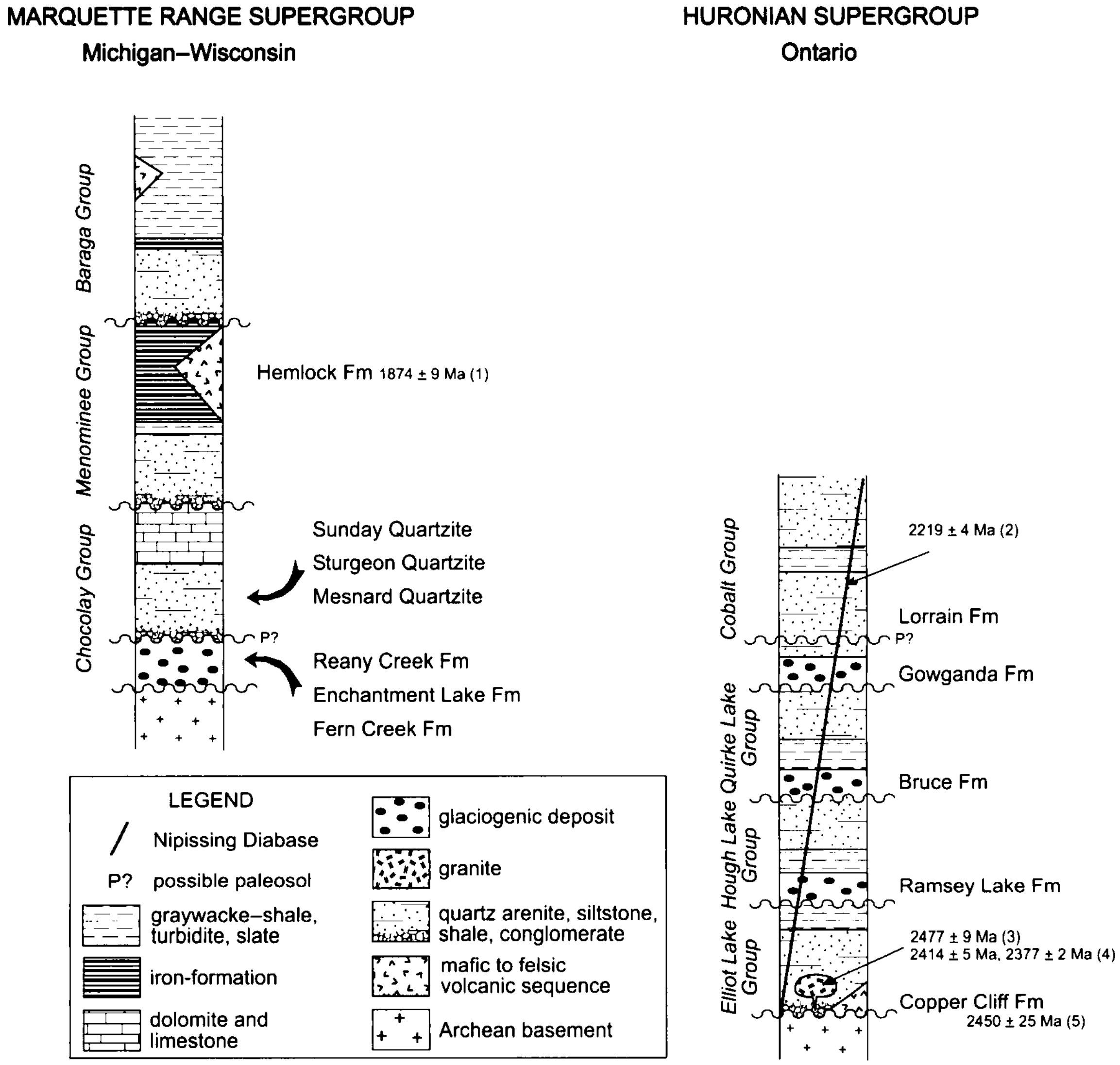

swarms in the North American provinces (e.g., Buchan et al. 1988, 1993, 1996; Roscoe and Card 1993). In the vicinity of Lake Superior, examples include the 2076^{+5}_{-4} Ma Fort Frances mafic dyke swarm in northern and western Minnesota, and adjacent Ontario (Southwick and Day 1983; Wirth et al. 1995; Buchan et al. 1996), the 2121^{+14}_{-7} Ma Marathon dykes north of Lake Superior, Ontario (Buchan et al. 1996), and the 2167 ± 2 Ma Biscotasing swarm east of Lake Superior, Ontario (Buchan et al. 1993), close to the Nipissing diabase.

The Penokean orogeny (1.87–1.83 Ga, Van Schmus 1976) occurred in the Lake Superior Region during collision of the southern margin of the Superior craton with the accreting arcs of the Wisconsin magmatic terranes (Sims et al. 1989, fig. 1). Intense deformation and metamorphism occurred in the fold and thrust belt that developed near the suture (the Niagara fault zone, Fig. 3), whereas a regional weak foliation and greenschist-facies metamorphism developed within the foreland basin to the north. Following the Penokean orogeny, a period of gneiss doming occurred at about 1.75 Ga just north of the Niagara fault zone that remobilized and deformed Archean basement rocks and overlying Paleoproterozoic (Schneider et al. 1996, 2004: Tinkham and Marshak 2004). Most of the region remained stable after this time. But the southernmost part of the region, including the Menominee Range, is believed to have been structurally reactivated during the Mazatzal orogeny at about 1.65–1.63 Ga (Romano et al. 2000). The final major tectonic episode in the region was formation of the Midcontinent Rift at ~1.1 Ga.

Analytical techniques and sample description

Hand-size outcrop samples of the Chocolay Group were analyzed in this study: three from the Enchantment Lake Formation (sample EL1-3), eight from the Sturgeon Quartzite (sample StQ1-8), and nine from the Sunday Quartzite (sample SuQ1-9). Sample localities are given in Table 1 and shown in Fig. 3. Polished thin-sections were examined by polarizing

Fig. 3. Generalized Early Proterozoic geology of the eastern part of the Lake Superior Region (from Schneider et al. 2002). The Chocolay Group was sampled from rare exposures around the base of the iron ranges of the younger Menominee Group shown in this figure. *EL*, Enchantment Lake Formation; *StQ*, Sturgeon Quartzite; *SuQ*, Sunday Quartzite.

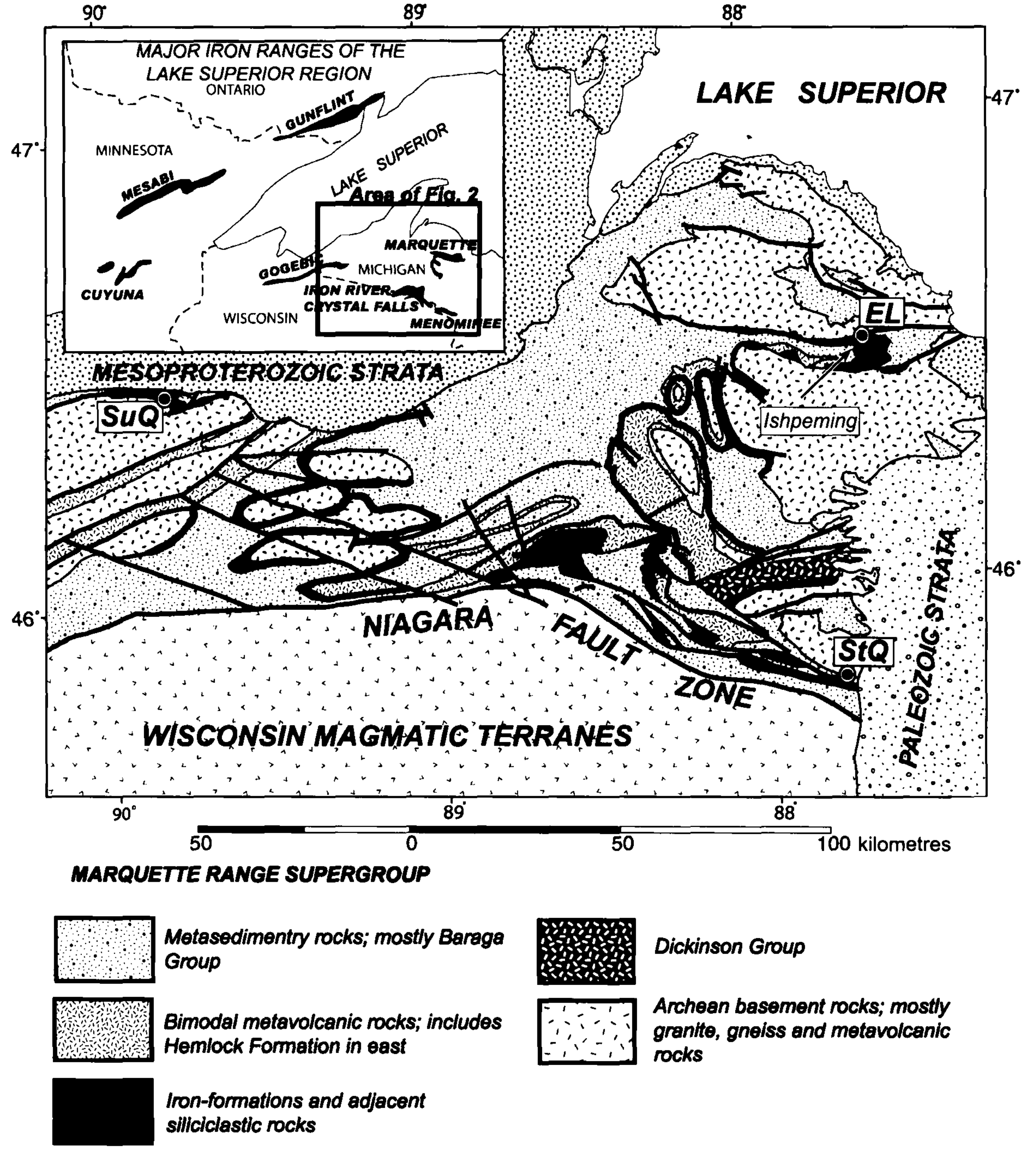

microscope and high-resolution backscattered scanning electron microscopy on a JEOL JSM-6400 scanning electron microscope, equipped with a Link Systems energy dispersive X-ray microanalyzer used for qualitative analysis. Operating conditions were 15–20 kV accelerating voltage and 3 nA beam current.

Uranium–Pb SHRIMP data were collected from detrital zircons. Zircons were separated from small crushed samples using standard heavy liquid and magnetic separation techniques. They were mounted in epoxy resin with several chips of the CZ3 standard zircon (U–Pb standard age of 564 Ma, Nelson 1997). Each mount was polished to expose the longitudinal midsection of the zircon grains. Session details (i.e., number of sessions and dates of sessions) are given in Table 2. Analytical procedures followed those published in Smith et al. (1998). Zircon $^{207}Pb/^{206}Pb$ data were used for age calculations. Data that were > 5% discordant were not considered sufficiently reliable and were not used in age calculations. To minimize the effect of common Pb, all analyses with 4f206 (i.e., 206Pb from common Pb) > 0.25% were not used in the age calculations.

Age data were grouped statistically using Isoplot (Ludwig

Table 1. Sample localities.

Sample Identifier	Formation	Location	Figs. 1, 3 labels
EL	Enchantment Lake Formation Chocolay Group	46°30′46″N, 87°36′06″W[a] NE Negaunee Marquette Range Marquette County Michigan	1
StQ	Sturgeon Quartzite Chocolay Group	45°47′21″N, 87°47′01″W[b] Sturgeon River area Dickinson County Michigan	3
SuQ	Sunday Quartzite Chocolay Group	46°27′58″N, 89°51′06″W[c] E–SE of Sunday Lake and Wakefield Gogebic Range Gogebic County Wisconsin	3

[a]United States Geological Survey (1985).
[b]United States Geological Survey (1982).
[c]United States Geological Survey (1990).

2001). This method does not distinguish zircon grains of different origin that have the same or similar age, within analytical uncertainty. In estimating the maximum age of sedimentation from the youngest detrital zircon population, we utilized the mean square of weighted deviates (MSWD) values from 1.0, the notional MSWD for an ideal Gaussian distribution, to 2.0, the approximate upper limit for real, but minor, scatter in ages about an ideal Gaussian distribution. Population ages and uncertainties were determined using Isoplot are statistical entities and may only approximate the ages of source terrains.

Uranium–Pb SHRIMP data were also collected from xenotime crystals. Plugs (3 mm diameter) containing selected xenotime crystals were drilled out of polished thin sections and mounted in epoxy resin disks for in situ analysis. Separate standard mounts were cleaned and gold coated simultaneously with the sample mounts prior to analysis. The primary U–Pb standard was MG-1 (U–Pb standard age of 490 Ma). The secondary standards were BS-1 (U–Pb standard age of 508 Ma), which monitored matrix corrections, and XENO-1 (U–Pb standard age of 994 Ma), which monitored both matrix corrections and $^{207}Pb/^{206}Pb$ (Fletcher et al. 2004). SHRIMP analytical procedures and matrix corrections for REE, U, and Th followed those published in Fletcher et al. (2000, 2004). Uncertainties in the tabulated and plotted data included all identified sources of random error, and are quoted at 1σ, whereas ages from pooled data are quoted with 95% confidence limits. All ages quoted in text and figures are $^{207}Pb/^{206}Pb$ ages.

Enchantment Lake Formation

Samples were collected in the eastern Marquette Range, Michigan (Table 1; Figs. 1, 3) and were taken ~2 m below the contact with the Mesnard Quartzite. Fine- to medium-grained quartzite beds (2–20 cm thick) are interbedded with thick beds of slate and belong to the quartzite–slate member described by Gair (1975). The quartzite contains micaceous, heavy mineral lamina spaced > 0.5 cm apart.

Sturgeon Quartzite

Quartzite samples were collected from the Menominee Range, Michigan (Table 1; Figs. 1, 3) and were taken within several metres above the contact (not exposed) with the underlying Fern Creek Formation. The quartzite is relatively pure and coarse-grained; however, the presence of some feldspar grains suggests it is not completely mature. The quartzite shows cross-lamination and ripple marks preserved on the upper faces of some beds, as well as the partial development of a weak foliation.

Sunday Quartzite

Samples of a sericite-rich, coarse-grained quartzite from the Gogebic Range, Michigan (Table 1; Figs. 1, 3), were taken from ~1 to 2 m above the contact between the Sunday Quartzite and underlying Archean granite. The quartzite shows planar- and cross-bedding (1–2 cm thick) defined by micaceous laminations.

Detrital zircon geochronology

Petrography

Enchantment Lake Formation

Zircon grains are clear, pale pink in colour, 100–250 µm in length, and range in shape from subhedral, elongate grains having at least two straight edges (length/breadth (*l*/*b*) = 2.5, Figs. 4*a*–4*c*) to euhedral, needle-like grains (*l*/*b* = 6, Fig. 4*d*). Less common are round, almost elliptical grains, some of which appear metamict and were avoided in SHRIMP analyses. Euhedral compositional zonation is common (Figs. 4*a*–4*d*).

Sturgeon Quartzite
Zircon grains are clear, colourless to pale brown in colour, 100–300 μm in length, and range from elongate grains with rounded edges (*l*/*b* = 2.5, Figs. 4*e*–4*g*) to subhedral grains with at least two straight edges (*l*/*b* = 2.5, Fig. 4*h*). Euhedral compositional zonation is common (Figs. 4*e*–4*h*).

Sunday Quartzite
Zircon grains are clear, pale brown in colour, 50–250 μm in length, and range in shape from the more common round, almost elliptical grains (*l*/*b* = 1.3, Figs. 4*i*–4*k*) to subhedral, elongate grains with at least two straight edges (*l*/*b* = 1.9, Fig. 4*l*). Euhedral compositional zonation is common (Figs. 4*i*–4*l*).

SHRIMP U–Pb results

The SHRIMP data for the detrital zircon suite in each formation are listed in Table 2. A cumulative probability plot displaying > 95% concordant detrital zircon data for each formation is shown in Fig. 5.

Enchantment Lake Formation
There is one main peak in the age data in the cumulative frequency plot in Fig. 5*a*; less than or equal to four analyses constitute the smaller peaks (Table 2). The dominant peak at ~2.3 Ga has a clearly defined curve on the younger side, whereas two small age peaks (each of two analyses, Table 2, Fig. 5*a*) are attached to the older side, which probably represent age mixtures between the ~2.3 Ga population and one at ~2.4 Ga (Fig. 4*b*). The 20 youngest analyses form the ~2.3 Ga peak (<5% discordant, Table 2), which is considered to represent a single population with a weighted mean age of 2317 ± 6 Ma (MSWD = 1.18, Fig. 6*a*). Zircon grains recording this age range in morphology from the euhedral, needle-like grains (Fig. 4*d*) to the subhedral, elongate grains (Fig. 4*c*), and are potentially of different origin. There are no analyses younger than this population. There appears to be an older population at ~2.7 Ga (four analyses), with some single analyses up to ~2.8 Ga (Fig. 5*a*). The older zircon grains are subhedral and elongate in shape (Fig. 4*a*).

Sturgeon Quartzite
A wider spread in age data was recorded from these zircon grains (Table 2), with at least two main age peaks in the cumulative frequency plot in Fig. 5*b*. There is a clustering of data at ~2.3 Ga that is inferred to be a discrete population, based on the sharp nature of the younger side of the curve and its complete separation from the remainder of the data (Table 2, Fig. 5*b*). The six youngest analyses (<5% discordant, Table 2) give a weighted mean age of 2306 ± 9 Ma (MSWD = 1.7, Fig. 6*b*). The zircon grains recording this age are subhedral and elongate in shape (Fig. 4*h*). There are minor peaks at ~2.5 Ga, ~2.56, ~2.67 Ga (each of two to five analyses, Table 2, Fig. 4*g*) that represent either discrete source regions or age mixtures between the apparent peak around 2.7 Ga and a younger population, such as that at ~2.3 Ga. Twelve analyses that constitute the double peak at ~2.7 Ga give a mean age of 2710 ± 6 Ma (MSWD = 2.0). The small peaks at ~2.75 Ga, ~2.78 Ga, and ~2.83 Ga (each of two to four analyses, Fig. 5*b*) either represent discrete source regions or age mixtures between the ~2.7 Ga peak and an older population, possibly represented by one of the single analyses between ~3.2 and 2.9 Ga (Fig. 5*b*). Zircon grains recording ages between 2.8 and 2.5 Ga are elongate with either rounded (Fig. 4*f*) or subhedral edges; those recording > 2.9 Ga are larger in size (Fig. 4*e*).

Sunday Quartzite
The cumulative frequency plot in Fig. 5*c* shows a narrow range in the data set that may, or may not, be a function of the smaller sample size when compared with the other two formations (Table 2). There is one main peak at ~2.65 Ga (Figs. 4*l*, 5*c*), which has a clearly defined young side and some tailing of data on its older side caused by six analyses between 2.95 and 2.67 Ga (Table 2, Figs. 4*j*–4*k*;). If the ~2.65 Ga peak is considered a single and the youngest population, the weighted mean age is 2647 ± 5 Ma (*n* = 8, MSWD = 1.4, Table 2). There is also a single analysis at ~2.79 Ga (Table 2; Figs. 4*i*, 5*c*).

Xenotime geochronology

Petrography

Enchantment Lake Formation
Authigenic xenotime is fairly abundant, with an average of 35 xenotime crystals per thin section (total of 15 thin sections), probably owing to the concentration of detrital zircon grains in heavy mineral laminations. The maximum size recorded was 40 μm but the average is 6 μm, and many xenotime crystals appear to have been destroyed by weathering or dissolution. Xenotime occurs as euhedral to irregular overgrowths on detrital zircon grains (Fig. 7*a*), as cement within cracks in zircon grains (Fig. 7*b*), and as replacements of inclusions within zircon grains (Fig. 7*c*).

Sturgeon Quartzite
Authigenic xenotime is very rare (approximately one xenotime crystal per thin section in a total of 10 thin sections). Xenotime occurs as ≤10 μm euhedral to irregular overgrowths on detrital zircon grains (Figs. 7*d*–7*e*).

Sunday Quartzite
Authigenic xenotime is not abundant (approximately four xenotime crystals per thin section in a total of 10 thin sections). Xenotime occurs as ≤10 μm euhedral to irregular overgrowths on detrital zircon grains (Figs. 7*g*–7*h*). A cluster of ~100 μm wide euhedral xenotime crystals within a detrital intraclast was also observed (Fig. 7*f*).

SHRIMP U–Pb results

Xenotime SHRIMP data are given in Table 3, and single lines on the zircon spectra in Fig. 5 represent xenotime analyses for each formation. Analyses with >10% discordance are not considered in the interpretation.

Enchantment Lake Formation
Five xenotime analyses with < 10% discordance were obtained (Table 3). The irregular xenotime overgrowth on zircon grain in Fig. 7*a* records two ages of 2458 ± 11 and 2462 ± 12 Ma that are within error. Xenotime cement in cracks in the zircon grain in Fig. 7*b* records two ages of

Table 2. SHRIMP U–Pb age data for detrital zircons from Enchantment Lake Formation, Sturgeon Quartzite, and Sunday Quartzite.

Analysis[a]	U (ppm)	Th (ppm)	$4f^{206}$ (%)[b]	$\frac{^{207}Pb}{^{206}Pb}$	±	$\frac{^{206}Pb}{^{238}U}$	±	$\frac{^{207}Pb}{^{235}U}$	±	$\frac{^{208}Pb}{^{232}Th}$	±	% Conc[c]	$t\left(\frac{^{207}Pb}{^{206}Pb}\right)$(Ma)	± (Ma)
Enchantment Lake Formation, < 5% discordant														
b17_1	80	37	0.18	0.1961	0.0015	0.567	0.011	15.33	0.33	0.1528	0.0040	104	2794	13
a15_1	91	91	0.00	0.1927	0.0012	0.512	0.010	13.81	0.28	0.1414	0.0030	98	2765	10
a25_1	32	21	0.00	0.1901	0.0019	0.536	0.013	14.04	0.36	0.1500	0.0042	101	2743	17
a2_1	35	32	0.07	0.1845	0.0018	0.512	0.011	13.01	0.31	0.1392	0.0037	99	2694	16
b20_2	82	59	0.08	0.1834	0.0013	0.502	0.010	12.70	0.27	0.1258	0.0034	98	2684	12
b8_1	194	83	0.04	0.1836	0.0008	0.493	0.009	12.49	0.24	0.1358	0.0027	96	2686	7
b14_1	118	63	0.06	0.1828	0.0013	0.505	0.010	12.73	0.26	0.1342	0.0029	98	2678	12
a3_1	198	121	0.00	0.1563	0.0007	0.445	0.008	9.60	0.18	0.1221	0.0024	98	2416	7
a10_1	242	87	0.00	0.1551	0.0007	0.437	0.008	9.33	0.17	0.1222	0.0024	97	2402	7
b3_1	179	57	0.03	0.1530	0.0008	0.431	0.008	9.09	0.18	0.1209	0.0027	97	2380	9
b4_1	160	81	0.03	0.1518	0.0008	0.433	0.008	9.06	0.18	0.1184	0.0025	98	2366	9
b2_1	20	8	0.00	0.1502	0.0026	0.427	0.011	8.84	0.27	0.1260	0.0046	98	2348	30
a21_2	86	49	0.00	0.1492	0.0011	0.418	0.008	8.61	0.18	0.1166	0.0027	96	2337	13
b25_1	168	104	0.08	0.1490	0.0008	0.428	0.008	8.78	0.17	0.1201	0.0025	98	2335	10
a21_4	73	41	0.11	0.1484	0.0013	0.440	0.009	9.01	0.21	0.1182	0.0030	101	2327	15
b18_1	120	48	0.04	0.1482	0.0010	0.427	0.008	8.73	0.18	0.1169	0.0026	99	2325	11
a30_1	115	46	0.02	0.1482	0.0011	0.444	0.009	9.08	0.19	0.1211	0.0027	102	2325	13
b11_1	228	115	0.10	0.1482	0.0008	0.432	0.008	8.82	0.17	0.1200	0.0024	100	2325	9
b10_1	240	167	0.07	0.1481	0.0007	0.426	0.008	8.70	0.16	0.1176	0.0023	98	2324	8
b28_1	135	95	0.01	0.1475	0.0010	0.424	0.008	8.63	0.17	0.1226	0.0026	98	2318	11
b9_1	150	61	0.14	0.1476	0.0010	0.440	0.008	8.95	0.18	0.1223	0.0028	101	2318	11
b1_1	224	157	0.17	0.1472	0.0009	0.420	0.008	8.53	0.16	0.1034	0.0021	98	2314	10
b13_1	277	133	0.05	0.1472	0.0006	0.436	0.008	8.85	0.17	0.1196	0.0025	101	2314	8
b26_1	169	106	0.09	0.1469	0.0009	0.409	0.008	8.23	0.17	0.1178	0.0025	95	2310	11
a22_1	167	74	0.08	0.1468	0.0008	0.405	0.008	8.20	0.16	0.1089	0.0023	95	2309	10
a21_3	89	53	0.13	0.1466	0.0011	0.418	0.008	8.46	0.18	0.1129	0.0025	98	2307	13
b23_1	77	52	0.20	0.1465	0.0015	0.418	0.008	8.44	0.19	0.1050	0.0028	98	2306	17
b7_1	248	125	0.07	0.1462	0.0007	0.415	0.008	8.36	0.16	0.1182	0.0024	97	2302	8
a29_1	233	245	11.97	0.1459	0.0197	0.445	0.011	8.94	1.22	0.1237	0.0164	103	2298	232
b24_1	148	113	0.11	0.1458	0.0010	0.443	0.008	8.90	0.18	0.1208	0.0026	103	2297	12
a21_1	77	44	0.14	0.1450	0.0012	0.426	0.009	8.51	0.19	0.1126	0.0027	100	2288	15
Enchantment Lake Formation, > 5% discordant														
b22_1	142	73	0.04	0.1886	0.0011	0.484	0.009	12.58	0.25	0.1378	0.0030	93	2730	9
b26_1	243	103	0.17	0.1864	0.0009	0.402	0.007	10.33	0.19	0.1568	0.0032	75	2711	8
b20_1	103	47	0.05	0.1848	0.0011	0.468	0.009	11.92	0.24	0.1414	0.0031	91	2697	10
a16_1	294	169	0.1	0.1643	0.0007	0.377	0.007	8.54	0.16	0.1183	0.0023	79	2501	8
b15_1	302	109	0.06	0.1634	0.0007	0.357	0.006	8.05	0.15	0.1119	0.0022	74	2491	7

Table 2 (*continued*).

Analysis[a]	U (ppm)	Th (ppm)	$4f^{206}$ (%)[b]	$\frac{^{207}Pb}{^{206}Pb}$	±	$\frac{^{206}Pb}{^{238}U}$	±	$\frac{^{207}Pb}{^{235}U}$	±	$\frac{^{208}Pb}{^{232}Th}$	±	% Conc[c]	$t\left(\frac{^{207}Pb}{^{206}Pb}\right)$(Ma)	± (Ma)
Enchantment Lake Formation, > 5% discordant														
a.11_1	379	129	0.02	0.1633	0.0007	0.265	0.005	5.97	0.11	0.0998	0.0019	36	2490	7
a13_1	240	142	0.34	0.1620	0.0010	0.333	0.006	7.43	0.14	0.0803	0.0018	66	2476	11
a14_1	272	223	0.46	0.1591	0.0011	0.317	0.006	6.96	0.13	0.1009	0.0022	62	2446	12
b6_1	129	46	0.08	0.1572	0.0012	0.428	0.008	9.27	0.19	0.1136	0.0032	94	2426	13
a7_1	330	134	0.08	0.1538	0.0007	0.344	0.006	7.29	0.14	0.1170	0.0023	75	2389	8
a4_1	431	214	1	0.1529	0.0014	0.402	0.007	8.47	0.17	0.1900	0.0040	91	2378	16
a23_1	557	241	0.09	0.1504	0.0007	0.193	0.003	3.99	0.07	0.0664	0.0013	93	2350	8
b21_1	165	65	0.02	0.1497	0.0008	0.405	0.008	8.35	0.16	0.1204	0.0025	93	2343	10
a20_1	614	151	0.62	0.1496	0.0013	0.131	0.002	2.7	0.05	0.0776	0.0019	4	2342	14
a9_1	530	286	0.72	0.1493	0.0012	0.257	0.005	5.29	0.10	0.1231	0.0024	42	2338	13
b20_1	194	81	-0.02	0.1491	0.0008	0.401	0.007	8.25	0.16	0.1167	0.0024	93	2336	9
b27_1	341	198	0.06	0.1488	0.0006	0.378	0.007	7.76	0.14	0.1199	0.0024	87	2333	7
a28_1	287	129	0.09	0.1488	0.0007	0.355	0.006	7.28	0.14	0.1030	0.0021	81	2332	8
b19_1	228	93	0.07	0.1487	0.0008	0.374	0.007	7.67	0.15	0.1136	0.0024	86	2331	9
b12_1	235	99	0.09	0.1481	0.0009	0.403	0.007	8.24	0.16	0.1206	0.0025	94	2324	10
a27_1	605	232	0.37	0.1480	0.0009	0.221	0.004	4.51	0.08	0.1147	0.0027	20	2323	11
a6_1	417	196	0.38	0.1479	0.0009	0.248	0.004	5.05	0.1	0.0785	0.0017	37	2322	11
a18_1	244	164	0.07	0.1475	0.0007	0.390	0.007	7.92	0.15	0.1144	0.0022	91	2317	8
a24_1	490	271	0.12	0.1469	0.0008	0.194	0.003	3.92	0.07	0.0497	0.0010	97	2310	9
a5_1	190	109	0.13	0.1466	0.0008	0.374	0.007	7.56	0.15	0.1079	0.0043	87	2307	10
a17_1	235	169	0.16	0.1467	0.0008	0.338	0.006	6.83	0.13	0.963	0.0020	77	2307	9
a12_1	298	101	0.06	0.1465	0.0010	0.302	0.006	6.11	0.12	0.1053	0.0022	65	2305	12
a8_1	480	40	0.12	0.1462	0.0008	0.180	0.003	3.62	0.07	0.1217	0.0041	84	2302	10
b5_1	370	150	0.21	0.1462	0.0008	0.311	0.006	6.26	0.12	0.1251	0.0025	68	2302	9
a26_1	341	133	0.37	0.1459	0.0010	0.244	0.004	4.92	0.09	0.0776	0.0020	37	2299	12
b16_1	552	193	0.25	0.1421	0.0008	0.183	0.003	3.59	0.07	0.1214	0.0023	92	2253	9
a19_1	422	122	0.54	0.141	0.0013	0.224	0.004	4.37	0.09	0.1089	0.0034	28	2245	16
Sturgeon Quartzite, < 5% discordant														
D035-7_1[1]	76	73	0.09	0.2471	0.0015	0.608	0.010	20.71	0.37	0.1659	0.0031	97	3166	10
d16_1[3]	35	12	0.18	0.2236	0.0016	0.595	0.018	18.35	0.58	0.1553	0.0069	100	3007	12
d33_1[3]	181	57	0.01	0.2108	0.0006	0.576	0.017	16.76	0.48	0.1534	0.0046	101	2912	4
d32_1[3]	86	64	0.03	0.2018	0.0008	0.559	0.017	15.57	0.46	0.1460	0.0045	101	2841	7
d13_1[3]	77	69	0	0.2016	0.0009	0.548	0.016	15.22	0.45	0.1529	0.0046	99	2839	7
0351d4_1[2]	99	79	0.07	0.2003	0.0012	0.534	0.010	14.75	0.30	0.1385	0.0030	97	2829	10
D035-2_1[1]	93	68	0.19	0.1987	0.0014	0.537	0.009	14.71	0.26	0.1454	0.0029	98	2815	12
0351d3_1[2]	142	108	0.08	0.1947	0.0011	0.567	0.011	15.23	0.30	0.1602	0.0033	104	2782	9
d28_1[3]	66	60	0.04	0.1933	0.0010	0.571	0.017	15.20	0.46	0.1531	0.0048	105	2770	9

Table 2 (*continued*).

Analysis[a]	U (ppm)	Th (ppm)	$4f^{206}$ (%)[b]	$^{207}Pb/^{206}Pb$	±	$^{206}Pb/^{238}U$	±	$^{207}Pb/^{235}U$	±	$^{208}Pb/^{232}Th$	±	% Conc[c]	$t\left(\frac{^{207}Pb}{^{206}Pb}\right)$ (Ma)	± (Ma)
Sturgeon Quartzite, < 5% discordant														
d12_1[3]	72	36	0.08	0.1929	0.0011	0.519	0.015	13.81	0.48	0.1401	0.0047	97	2767	10
d18_1[3]	62	25	0.01	0.1908	0.0010	0.505	0.015	13.29	0.40	0.1376	0.0050	96	2749	9
d25_1[3]	88	96	0.01	0.1904	0.0008	0.547	0.016	14.36	0.42	0.1512	0.0045	102	2746	7
0351d3_1[2]	137	92	0.04	0.1882	0.0011	0.539	0.010	13.99	0.27	0.1509	0.0084	102	2726	10
d23_1[3]	65	27	0.04	0.1877	0.0010	0.513	0.015	13.28	0.40	0.1392	0.0048	98	2722	9
d34_1[3]	44	73	0.03	0.1875	0.0012	0.525	0.016	13.57	0.42	0.1417	0.0044	100	2721	11
d15_1[3]	93	94	0.00	0.1870	0.0008	0.532	0.016	13.72	0.41	0.1474	0.0046	101	2716	7
d11_1[3]	85	43	0.03	0.1869	0.0008	0.551	0.016	14.2	0.42	0.1482	0.0046	104	2715	7
d22_1[3]	82	83	0.00	0.1868	0.0009	0.516	0.015	13.29	0.39	0.1440	0.0043	99	2714	8
d19_1[3]	342	352	0.00	0.1868	0.0004	0.519	0.015	13.36	0.38	0.1443	0.0042	99	2714	4
D035-5_1[1]	74	64	0.00	0.1858	0.0014	0.503	0.008	12.88	0.24	0.1409	0.0028	97	2705	13
D035-3_1[1]	78	52	0.08	0.1854	0.0014	0.499	0.009	12.77	0.24	0.1380	0.0028	97	2702	12
D035-8_1[1]	85	78	0.40	0.1853	0.0018	0.503	0.008	12.84	0.24	0.1363	0.0055	97	2701	16
d26_1[3]	123	90	0.01	0.1849	0.0007	0.506	0.015	12.91	0.38	0.1372	0.0041	98	2698	6
d14_1[3]	199	147	0.05	0.1847	0.0005	0.508	0.015	12.94	0.37	0.1327	0.0041	98	2695	5
d21_1[3]	218	132	0.03	0.1839	0.0006	0.496	0.014	12.59	0.36	0.1381	0.0041	97	2688	5
d29_1[3]	46	22	0.73	0.1831	0.0030	0.540	0.016	13.63	0.46	0.1005	0.0083	104	2681	27
d36_1[3]	201	62	0.06	0.1819	0.0008	0.518	0.015	13.00	0.38	0.1461	0.0057	101	2670	7
d27_1[3]	186	87	0.10	0.1806	0.0008	0.499	0.014	12.43	0.36	0.1362	0.0041	98	2659	7
d17_1[3]	232	125	0.01	0.1805	0.0005	0.509	0.015	12.67	0.37	0.1404	0.0042	100	2657	5
d24_1[3]	96	71	0.08	0.1707	0.0007	0.500	0.015	11.77	0.35	0.1370	0.0042	102	2564	7
d24_2[3]	101	58	0.10	0.1705	0.0008	0.461	0.013	10.83	0.32	0.1303	0.0040	95	2563	8
D035-6_1[1]	228	88	0.00	0.1652	0.0008	0.489	0.007	11.14	0.17	0.1348	0.0023	102	2509	8
d37_1[3]	377	158	0.03	0.1639	0.0004	0.491	0.014	11.08	0.32	0.1369	0.0040	103	2496	4
d41_1[3]	65	35	0.00	0.1488	0.0010	0.463	0.014	9.50	0.29	0.1338	0.0044	105	2333	11
d38_1[3]	66	37	0.04	0.1473	0.0010	0.443	0.013	9.00	0.27	0.1247	0.0040	102	2315	11
d20_1[3]	76	40	0.01	0.1473	0.0008	0.439	0.013	8.92	0.27	0.1258	0.0040	101	2315	9
d39_1[3]	89	55	0.01	0.1466	0.0008	0.431	0.013	8.71	0.26	0.1194	0.0037	100	2306	9
d31_1[3]	339	149	0.00	0.1464	0.0004	0.444	0.013	8.96	0.26	0.1233	0.0037	103	2304	5
d40_1[3]	576	349	0.01	0.1462	0.0003	0.407	0.012	8.21	0.24	0.1136	0.0033	95	2302	4
Sturgeon Quartzite, > 5% discordant														
D035-4_1[1]	77	50	0.32	0.2022	0.0019	0.478	0.008	13.33	0.26	0.1036	0.0030	87	2844	15
D035-9_1[1]	199	186	0.35	0.1904	0.0011	0.392	0.006	10.29	0.18	0.1179	0.0021	71	2746	10
D035-1_1[1]	208	40	0.15	0.1879	0.0010	0.465	0.007	12.06	0.19	0.1182	0.0038	89	2724	9
d30_1[3]	165	151	0.08	0.1877	0.0007	0.372	0.011	9.62	0.28	0.0965	0.0029	66	2722	7
d35_1[3]	120	94	0.04	0.1863	0.0008	0.466	0.013	11.96	0.35	0.1260	0.0038	90	2710	7
0351d1_1[2]	318	115	0.09	0.1659	0.0007	0.448	0.008	10.24	0.18	0.1252	0.0025	94	2516	7

Table 2 (*concluded*).

Analysis[a]	U (ppm)	Th (ppm)	$4f^{206}$ (%)[b]	$^{207}Pb/^{206}Pb$	±	$^{206}Pb/^{238}U$	±	$^{207}Pb/^{235}U$	±	$^{208}Pb/^{232}Th$	±	% Conc[c]	$t\left(\frac{^{207}Pb}{^{206}Pb}\right)$ (Ma)	± (Ma)
Sturgeon Quartzite, > 5% discordant														
D035-10_1[1]	318	114	0.19	0.1642	0.0007	0.421	0.006	9.52	0.14	0.1214	0.0021	90	2499	7
0351d1_1[2]	412	458	0.16	0.1613	0.0007	0.396	0.007	8.80	0.16	0.0470	0.0009	85	2469	8
Sunday Quartize, < 5% discordant														
b6_1[2]	98	42	0.13	0.1957	0.0010	0.517	0.015	13.93	0.41	0.1329	0.0043	96	2790	8
b19_1[2]	24	17	0.00	0.1846	0.0017	0.524	0.016	13.33	0.43	0.1449	0.0055	101	2695	15
0351b2_1[1]	100	22	0.02	0.1841	0.0013	0.499	0.010	12.66	0.26	0.1443	0.0047	97	2689	12
b7_1[2]	156	49	0.00	0.1837	0.0006	0.524	0.015	13.27	0.38	0.1469	0.0045	101	2686	6
b9_1[2]	32	7	0.19	0.1828	0.0016	0.494	0.015	12.44	0.40	0.1408	0.0067	96	2678	15
b18_1[2]	112	26	0.00	0.1823	0.0008	0.503	0.019	12.64	0.49	0.1360	0.0083	98	2674	7
b14_1[2]	175	48	0.04	0.1820	0.0006	0.519	0.015	13.02	0.38	0.1462	0.0046	101	2671	5
b10_1[2]	177	145	0.00	0.1810	0.0006	0.506	0.015	12.63	0.37	0.1397	0.0041	99	2662	5
b12_1[2]	245	158	0.05	0.1804	0.0005	0.440	0.013	10.95	0.32	0.1103	0.0032	87	2657	5
b13_2[2]	123	89	0.02	0.1800	0.0008	0.490	0.014	12.16	0.36	0.134	0.0041	97	2653	7
b3_1[2]	331	264	0.03	0.1796	0.0005	0.501	0.014	12.40	0.36	0.1362	0.0040	99	2649	4
b15_1[2]	227	66	0.00	0.1791	0.0005	0.515	0.015	12.72	0.37	0.1435	0.0043	101	2645	5
b17_1[2]	26	8	0.46	0.1789	0.0030	0.489	0.016	12.08	0.48	0.1272	0.0079	97	2643	28
b11_1[2]	248	103	0.05	0.1788	0.0005	0.502	0.014	12.38	0.38	0.1380	0.0041	99	2642	5
b15_2[2]	206	56	0.01	0.1788	0.0005	0.521	0.015	12.83	0.37	0.1434	0.0043	102	2642	5
b13_1[2]	116	83	0.08	0.1783	0.0007	0.520	0.015	12.79	0.37	0.1410	0.0042	102	2637	7
Sunday Quartize, > 5% discordant														
0351b1_1[1]	824	56	0.08	0.2671	0.0005	0.5610	0.0095	20.61	0.35	0.1380	0.0053	86	3285	3
b5_1[2]	197	196	0.21	0.1833	0.0009	0.4716	0.0135	11.92	0.35	0.1390	0.0049	92	2683	8
b16_1[2]	99	111	0.00	0.1820	0.0009	0.4781	0.0140	11.10	0.36	0.1327	0.0042	94	2671	8
b8_1[2]	86	40	0.07	0.1819	0.0010	0.5651	0.0166	14.17	0.42	0.1510	0.0050	108	2670	9
b4_1[2]	114	103	0.00	0.1813	0.0007	0.4608	0.0133	11.51	0.34	0.1279	0.0038	91	2665	6

Note: All precisions are 1σ. U/Pb systematic reproducibility propagated from CZ3 standards for Mount 04-79 is 0.52% (n = 14); for Mount 03-51 it is 0.48% (n = 12) on 13 July 2003, 1.34% (n = 4) on 24 January 2004, and 0.71% (n = 19) on 2 February 2004. U–Pb standard age for CZ3 is 564 Ma (Nelson 1997).

[a]SHRIMP analysis number and letter combination refers to the grain identification; grains with multiple spots have a second identification number. [1,2,3] refers to the session. Enchantment Lake Formation zircons (Mount 04-79) were analyzed on 24 July 2004. Sturgeon Quartzite zircons (Mount 03-51) were analyzed on 13 July 2003, 24 January 2004, and 2 February 2004. Sunday Quartzite zircons (Mount 03-51) were analyzed on 24 January 2004 and 2 February 2004.

[b]$4f^{206}$(%) = % of ^{206}Pb which is owing to common Pb. All Pb isotope data are corrected for common Pb, using measured ^{204}Pb and the isotopic composition of Broken Hill galena.

[c]%Concordance (%Conc) = 100 × [$t(^{206}Pb/^{238}U)/t(^{207}Pb/^{206}Pb)$], where t = time.

Fig. 4. Cathodoluminescence images of detrital zircon grains that are representative of each of the petrographic types and ages within each zircon suite. SHRIMP analysis spots are labelled with identification and age (see Table 2). Enchantment Lake Formation: (*a*) subhedral zircon grain of 2765 ± 10 Ma; (*b*) subhedral zircon grain of 2402 ± 7 Ma; (*c*) subhedral zircon grain of 2309 ± 10 Ma; (*d*) euhedral, needle-like zircon grain of 2314 ± 10 Ma. Sturgeon Quartzite: (e) rounded zircon grain of 3166 ± 10 Ma; (*f*) subhedral zircon grain of 2701 ± 18 Ma; (*g*) rounded zircon grain of 2496 ± 4 Ma; (*h*) subhedral zircon grain of 2315 ± 9 Ma. Sunday Quartzite: (*i–l*) rounded to subhedral zircon grains of 2790 ± 8, 2686 ± 8, 2678 ± 15, and 2642 ± 5 Ma, respectively.

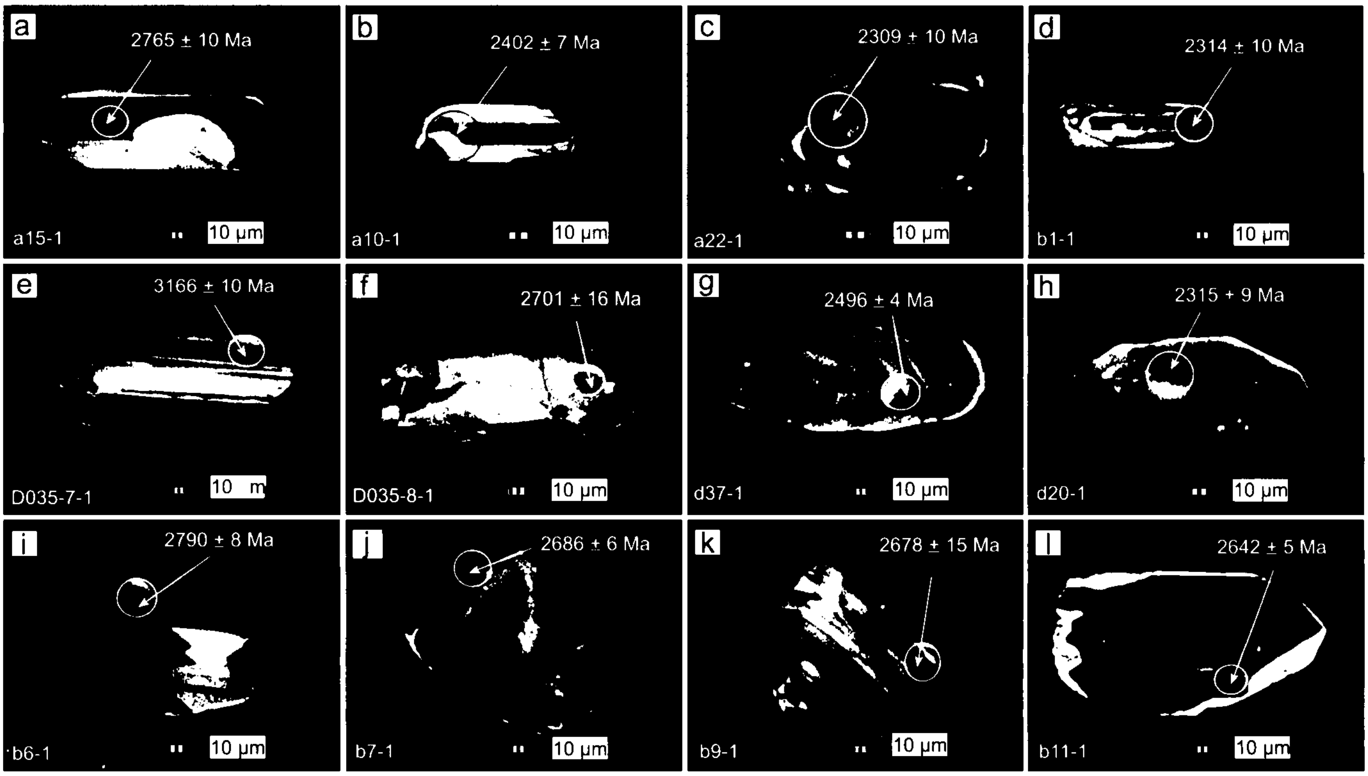

2133 ± 11 and 2131 ± 13 Ma, also within error, and xenotime replacement of the inclusion in the zircon grain in Fig. 7*c* records an age of 2019 ± 35 Ma. This last age has a $4f^{206}$ value > 0.25% and is not discussed further.

Sturgeon Quartzite

The xenotime overgrowth on zircon grain in Fig. 7*d* records an age of 2584 ± 7 Ma, whereas the xenotime overgrowth on zircon grain in Fig. 7*e* records an age of 2115 ± 5 Ma.

Sunday Quartzite

The cement-like xenotime crystal in the detrital intraclast in Fig. 7*f* records three ages of 2582 ± 7, 2558 ± 5, and 2596 ± 3 Ma. The euhedral xenotime overgrowth on zircon grain in Fig. 7*g* records an age of 2405 ± 5 Ma. The irregular xenotime overgrowth on zircon grain in Fig. 7*h* records two ages of 2333 ± 3 and 2207 ± 5 Ma.

Interpretation of xenotime origin from petrography and geochronology

Xenotime crystals in the Enchantment Lake Formation, Sturgeon Quartzite, and Sunday Quartzite with ages ≥2.4 Ga (Figs. 7*a*, 7*d*, 7*f*, 7*g*) are detrital in origin (labelled as "d" in Fig. 5) because they are older than the youngest detrital zircon populations in both the Enchantment Lake Formation and Sturgeon Quartzite. It is also likely that the xenotime overgrowth on the zircon grain from the Sunday Quartzite, which records an age of ~2.3 Ga (Fig. 7*h*), represents part of a detrital crystal that was eroded and redeposited in the sediments of the Chocolay Group. The part of the crystal recording the ~2.2 Ga age represents younger xenotime growth that nucleated on the detrital grain after sedimentation.

Xenotime cement that filled cracks or replaced inclusions in zircon grains is atypical of the diagenetic pyramidal overgrowths on zircons (Rasmussen 1996) or the diagenetic pore-filling cement-like overgrowths on zircons (Vallini et al. 2002, 2005). Thus, the ~2.13 Ga (Fig. 7*b*) and possibly ~2.02 Ga (Fig. 7*c*) xenotime crystals in the Enchantment Lake Formation are likely to be hydrothermal or metamorphic. Texturally, the small irregular xenotime overgrowths on zircons in the Sturgeon Quartzite and Sunday Quartzite with ages of ~2.12 Ga (Fig. 7*e*) and ~2.2 Ga (Fig. 7*h*), respectively, also appear to be of hydrothermal or metamorphic origin. Kositcin et al. (2003) recorded xenotime overgrowths on detrital zircon and xenotime with similar textures in sediments from the Witwatersrand Basin in South Africa, which also were attributed to hydrothermal processes.

The small number of xenotime age determinations in this study, owing to the rarity of ≥10 µm xenotime crystals in these samples, makes it difficult to reliably determine if the ages for the hydrothermal xenotime crystals record discrete events or are a result of mixing between older and younger components. The two analyses, 2133 ± 11 and 2131 ±

Fig. 5. Cumulative frequency plots containing concordant age data from detrital zircon grains in the (*a*), Enchantment Lake Formation (n_z = 30), (*b*) Sturgeon Quartzite (n_z = 39), (*c*) Sunday Quartzite (n_z = 16). Single spot analyses from xenotime crystals (detrital crystals are labelled "d", see text) are added for reference.

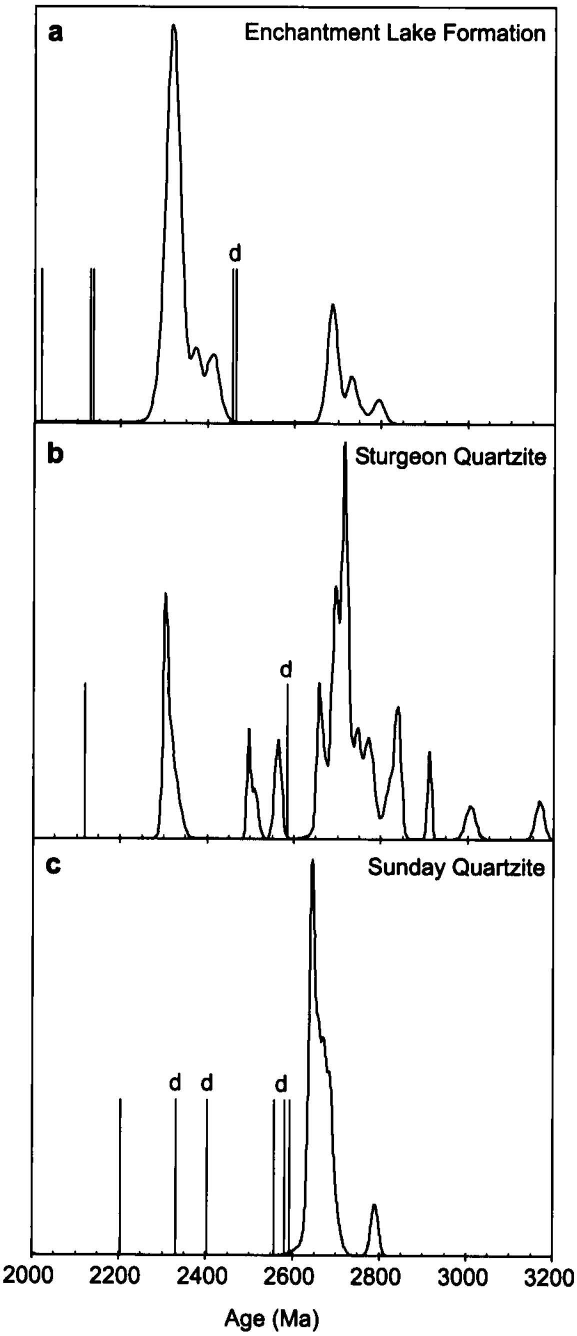

13 Ma, recorded from different sections of the same xenotime crystal in the Enchantment Lake Formation (Fig. 7*b*) suggest that at least this xenotime age records a discrete xenotime growth event at ~2.13 Ga.

Discussion

The new age constraints for the Chocolay Group presented here are not only significant for the geological history of the Michigan area but also have wider implications to the geological history of the Lake Huron and Lake Superior regions.

Fig. 6. Detrital zircon U–Pb concordia plots for the youngest zircon population in the (*a*), Enchantment Lake Formation, (*b*) Sturgeon Quartzite. MSWD, mean square of weighted deviates.

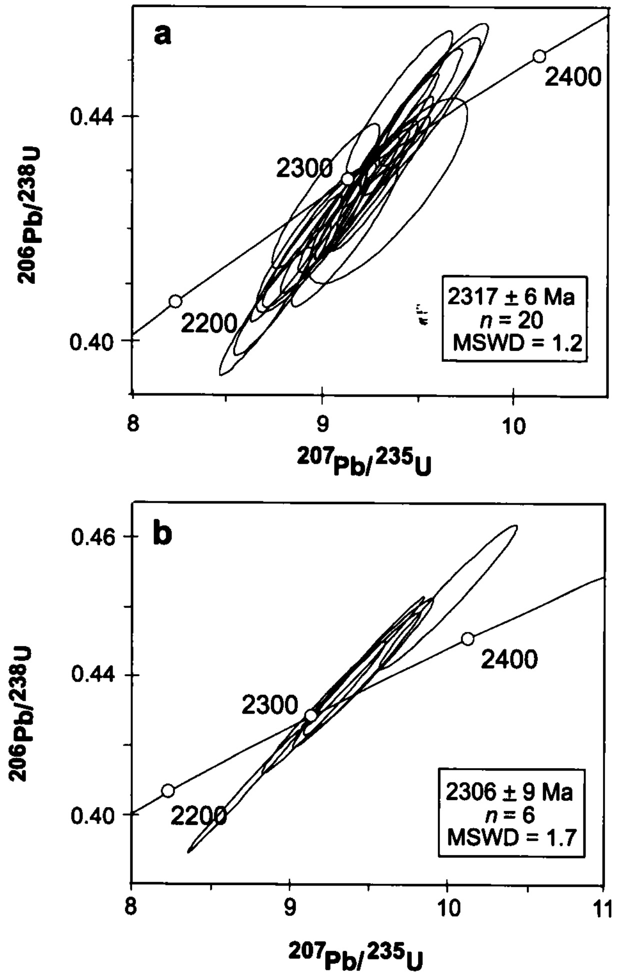

Chocolay Group depositional ages

The 2317 ± 6 Ma detrital zircon population in the Enchantment Lake Formation provides the maximum age of deposition for this formation. The hydrothermal xenotime age of ~2.13 Ga probably provides a minimum age. The 2306 ± 9 Ma detrital zircon population in the Sturgeon Quartzite provides the maximum age of deposition for this formation, as well as for its stratigraphic equivalent, the Sunday Quartzite. The hydrothermal xenotime ages of ~2.2 Ga and ~2.12 Ga from these formations probably provide minimum ages. Geological evidence (paleosols) indicates a period of weathering between the glaciogenic rocks and quartzite of the Chocolay Group. Our age data do not contradict this interpretation but show that the duration of this period must have been < ~100 million years.

The age of the Menominee Group was recently determined to be ~1.875 Ga by Schneider et al. (2002, fig. 2), and this study shows that the Chocolay Group must be older than ~2.13 Ma and possibly ~2.2 Ma. This leaves a hiatus of

Table 3. SHRIMP U–Pb age data for authigenic xenotime crystals from the Enchantment Lake Formation, Sturgeon Quartzite, and Sunday Quartzite.

Analysis[a]	U (ppm)	Th (ppm)	$4f^{206}$ (%)[b]	$\frac{^{207}Pb}{^{206}Pb}$	±	$\frac{^{206}Pb}{^{238}U}$	±	$\frac{^{207}Pb}{^{235}U}$	±	$\frac{^{208}Pb}{^{232}Th}$	±	% Conc[c]	$t\left(\frac{^{207}Pb}{^{206}Pb}\right)$(Ma)	± (Ma)
Enhancement Lake Formation, < 10% discordant														
dv114i1_2	792	2192	0.08	0.1606	0.0012	0.4296	0.0185	9.5109	0.0417	0.0838	0.0037	94	2462	12
dv114i1_1	999	2074	0.16	0.1602	0.0011	0.4551	0.0193	10.0535	0.0432	0.1146	0.0049	98	2458	11
0496F1_1	4310	87272	0.09	0.1326	0.0008	0.3700	0.0036	6.7673	0.0781	0.1090	0.0011	95	2133	11
0496F1_2	4517	96159	0.15	0.1325	0.0010	0.3316	0.0036	6.0562	0.0789	0.1084	0.0012	90	2131	13
113b1_1	545	2990	0.82	0.1243	0.0025	0.3675	0.0191	6.3008	0.0354	0.0979	0.0064	100	2019	35
Enhancement Lake Formation, >10% discordant														
114f1_1	116327	232331	1.71	0.1311	0.0058	0.0000	0.0046	0.0000	0.0000	0.0000	0.0000	6	2112	77
113b2_1	170	1328	0.26	0.1309	0.0017	0.4998	0.0267	9.0218	0.0499	0.1515	0.0098	124	2110	23
114a1_1	93612	119101	1.00	0.1307	0.0029	0.0000	0.0000	0.0000	0.0000	0.0000	0.0000	0	2108	38
114b1_1	34074	48682	1.25	0.1295	0.0032	0.0455	0.0038	0.8114	0.0076	0.0280	0.0031	14	2091	43
113i4_1	4898	16671	0.37	0.1270	0.0013	0.2295	0.0145	4.0172	0.0258	0.0881	0.0060	65	2057	18
113i5_1	2965	14709	0.38	0.1262	0.0023	0.2509	0.0190	4.3660	0.0343	0.1075	0.0098	71	2046	33
113h4_1	1957	18964	0.30	0.1256	0.0012	0.2261	0.0117	3.9159	0.0208	0.0854	0.0062	64	2038	17
113h5_1	2735	23177	0.43	0.1248	0.0014	0.1375	0.0075	2.3661	0.0132	0.0595	0.0035	41	2026	20
113i3_1	9364	35296	0.63	0.1234	0.0018	0.1251	0.0086	2.1280	0.0151	0.0490	0.0039	38	2006	26
113i2_1	12583	31469	1.29	0.1217	0.0036	0.1348	0.0084	2.2621	0.0164	0.0538	0.0072	41	1982	53
dv113h1_1	2238	16865	1.29	0.1202	0.0043	0.1270	0.0060	2.1037	0.0130	0.0899	0.0045	39	1959	63
113h2_1	2004	20518	0.60	0.1197	0.0015	0.1703	0.0088	2.8096	0.0150	0.0730	0.0094	52	1951	23
113a1_2	2838	19187	1.14	0.1188	0.0035	0.1792	0.0109	2.9357	0.0203	0.0665	0.0065	55	1938	52
113e1_2	16097	116149	1.81	0.1185	0.0033	0.0311	0.0038	0.5082	0.0068	0.0208	0.0035	10	1934	49
113i1_1	1542	12967	0.48	0.1180	0.0015	0.2376	0.0272	3.8680	0.0446	0.1173	0.0190	71	1927	22
113c1_1	3488	17735	0.46	0.1178	0.0017	0.1902	0.0098	3.0892	0.0167	0.0882	0.0097	58	1923	25
114d2_1	8593	71913	0.36	0.1178	0.0025	0.2419	0.0192	3.9283	0.0333	0.0966	0.0100	73	1923	37
113a1_1	9206	49106	0.59	0.1171	0.0027	0.1176	0.0080	1.8983	0.0142	0.0435	0.0041	37	1912	41
113h6_1	5517	28402	3.65	0.1169	0.0078	0.1364	0.0077	2.1996	0.0213	0.0599	0.0061	43	1910	120
113c3_1	3076	19820	0.70	0.1169	0.0018	0.0996	0.0055	1.6055	0.0093	0.0630	0.0050	32	1909	28
Sturgeon Quartzite, < 10% discordant														
0302G1_1	6709	16796	0.15	0.1727	0.0008	0.4814	0.0101	11.4608	0.0246	0.0941	0.0021	98	2584	7
0302E1_1	5518	7787	0.07	0.1313	0.0004	0.3694	0.0080	6.6883	0.0147	0.1065	0.0026	96	2115	5
Sunday Quartzite, < 10% discordant														
dv57m1_1	12216	12267	0.01	0.1740	0.0003	0.4555	0.0139	10.9285	0.0336	0.1289	0.0040	93	2596	3
0357M1_1	8880	7209	0.02	0.1725	0.0007	0.4536	0.0086	10.7861	0.0211	0.1342	0.0026	93	2582	7
0357M1_2	5135	4900	0.02	0.1700	0.0005	0.4722	0.0085	11.0706	0.0203	0.0965	0.0020	97	2558	5
0302H2_1	14259	14225	0.03	0.1553	0.0005	0.4947	0.0110	10.5913	0.0238	0.1233	0.0029	108	2405	5
0357J1_1	5519	4711	0.03	0.1489	0.0028	0.3851	0.0070	7.9063	0.0216	0.0809	0.0018	90	2333	32

Table 3. SHRIMP U–Pb age data for authigenic xenotime crystals from the Enchantment Lake Formation, Sturgeon Quartzite, and Sunday Quartzite.

Analysis[a]	U (ppm)	Th (ppm)	$4f_{206}$ (%)[b]	$^{207}Pb/^{206}Pb$	±	$^{206}Pb/^{238}U$	±	$^{207}Pb/^{235}U$	±	$^{208}Pb/^{232}Th$	±	% Conc[c]	$t\left(\frac{^{207}Pb}{^{206}Pb}\right)$ (Ma)	± (Ma)
dv57j1_1	6809	5748	0.04	0.1384	0.0004	0.4165	0.0119	7.9457	0.0230	0.0852	0.0025	102	2207	5
Sunday Quartzite, >10% discordant														
0302H1_1	21167	20584	0.05	0.1580	0.0005	0.3999	0.0096	8.7103	0.0211	0.1016	0.0025	89	2434	5
dv57k1_1	3771	5921	1.25	0.1431	0.0020	0.3174	0.0091	6.2652	0.0204	0.0592	0.0027	78	2266	24
0357J1_2	4802	5088	0.04	0.1367	0.0015	0.3160	0.0159	5.9569	0.0308	0.0541	0.0028	81	2186	19
dv57I1_1	7810	48160	0.17	0.1308	0.0008	0.0844	0.0030	1.5231	0.0056	0.0125	0.0005	25	2109	10
0357L1_1	4763	24060	0.13	0.1267	0.0009	0.0656	0.0073	1.1464	0.0128	0.0143	0.0018	20	2053	12

Note: All precisions are 1σ. U/Pb systematic reproducibility propagated from MG-1 standards for Mounts 03-113 and 03-114 is 4.6% (n = 8) on 29 February 2004 and 3.8% (n = 8) on 29 March 2004; for Mount 03-02, it is 1.9% (n = 8); for Mount 03-57, it is 1.7% (n = 10) on 14 December 2003. Reproducibility propagated from BS-1 standards for Mount 03-57 is 2.6% (n = 14) on 14 November 2003. U–Pb standard age is 490 Ma for MG-1, 508 Ma for BS-1, and 994 Ma for XENO-1 (Fletcher et al. 2002, 2004).

[a]SHRIMP spot analysis number and letter combination refers to the grain identification; grains with multiple spots have a second identification number. [1,2,3] refers to the session. Enchantment Lake Formation xenotime (Mount 03-113, Mount 03-114) was analyzed on the 29 February 2004 and 29 March 2004. Sturgeon Quartzite xenotime (Mount 03-02) was analyzed on 13 April 2003. Sunday Quartzite xenotime (Mount 03-02, Mount 03-57) was analyzed on 13 April 2003, 14 November 2003, and 14 December 2003.

[b]$4f_{206}$(%) = % of ^{206}Pb which is owing to common Pb. All Pb isotope data are corrected for common Pb, using measured ^{204}Pb and the composition of Broken Hill galena.

[c]%Concordance (%Conc) = 100 × [$t(^{206}Pb/^{238}U)/t(^{207}Pb/^{206}Pb)$)], where t = time.

up to 325 million years. between deposition of the Chocolay and Menominee groups.

The detrital zircon data in this study confirm that the Chocolay Group (2.3–2.2 Ga) correlates in time with some part of the Huronian sequence (2.45–2.22 Ga; Krogh et al. 1984; Corfu and Andrews 1986) in Ontario. The lack of tight age constraints for the Huronian Supergroup means that the glaciogenic formation in the Chocolay Group may still be correlated with the Ramsey Lake, Bruce, or Gowganda formations (Fig. 2). However, the mature quartzites above the glaciogenic rocks in the Chocolay Group are most similar to the mature quartzites (i.e., Lorrain and Bar River formations) above the Gowganda Formation in the Cobalt Group.

Chocolay Group sediment provenance

The zircon suite in the Enchantment Lake Formation was derived from at least two sources. Zircon grains with ages between 2.8 and 2.7 Ga are most likely sourced from the Archean greenstone–granite terranes of the Superior Province (Fig. 1). The source(s) of the ~2.3 Ga zircons remains an enigma. From the texture of the ~2.3 Ga euhedral, needle-like detrital zircon grains within the quartzite (Fig. 4*d*), it can be inferred that they were derived from a volcanic sequence(s) proximal to the site of deposition of the Enchantment Lake Formation because they could not have withstood long water transport distances. The subhedral, elongate zircon grains (Fig. 4*c*) of the same age may have had intrusive sources. The only known igneous rock unit close to the outcrop area of the Enchantment Lake Formation with an age of 2345 ± 20 Ma (U–Pb zircon, Hammond 1978) is a small granite pluton about 10 km^2 in area, which is exposed south of the town of Ishpeming, Michigan (Fig. 3). This granite intrudes Archean granitic and gneissic rocks, but it is not lithologically distinct from some phases of these Archean rocks; therefore, it can not be identified as a Paleoproterozoic intrusion based solely on field examination. This suggests the possibility that additional granite plutons of similar age may have existed in the area but have either not been recognized or do not outcrop.

The younger (2.377 ± 2 Ma; Smith 2002) phase of the Creighton granite that intrudes the Elliot Lake Group in Ontario is at least 400 km to the east (Fig. 1). Thus, the Enchantment Lake Formation may have been partly derived from the Huronian area, currently ~200 km to the east in Ontario (Fig. 1), or from equivalent rocks that were once more widespread. The Dickinson Group, whose exact age remains unknown, forms an easterly trending belt between the Menominee and Marquette ranges in Michigan (Fig. 3) and is inferred to predate the Marquette Range Supergroup (James et al. 1961). Unconformably overlying Archean granite gneiss, the sequence consists of arkose, conglomerate, schist, and amphibolite. The amphibolite represents the relic of a thick mafic volcanic series. The sequence is cut by granitic intrusions and the rocks are multiply deformed and metamorphosed. The lithology, metamorphic grade, and level of internal deformation of the rocks in the Dickinson Group do not resemble adjacent sequences of the Marquette Range Supergroup. Perhaps the Dickinson Group (or other deposits in Michigan since removed by erosion) is equivalent to units in the lower Huronian and provided the source material for the glaciogenic units of the Chocolay Group (e.g., needle-like

Fig. 7. Back-scattered electron images of each of the xenotime crystals analyzed with SHRIMP. Analysis spots are labelled with age and identification (see Table 3). (a–c) Enchantment Lake Formation xenotime crystals in the form of overgrowths on zircon grains, cement in cracks in zircon grains, and replacements of inclusions in zircon grains. (d–e) Sturgeon Quartzite xenotime crystals in the form of overgrowths on zircon grains. (f–h) Sunday Quartzite xenotime crystals in the form of large amalgamated crystals and euhedral to irregular overgrowths on zircon grains.

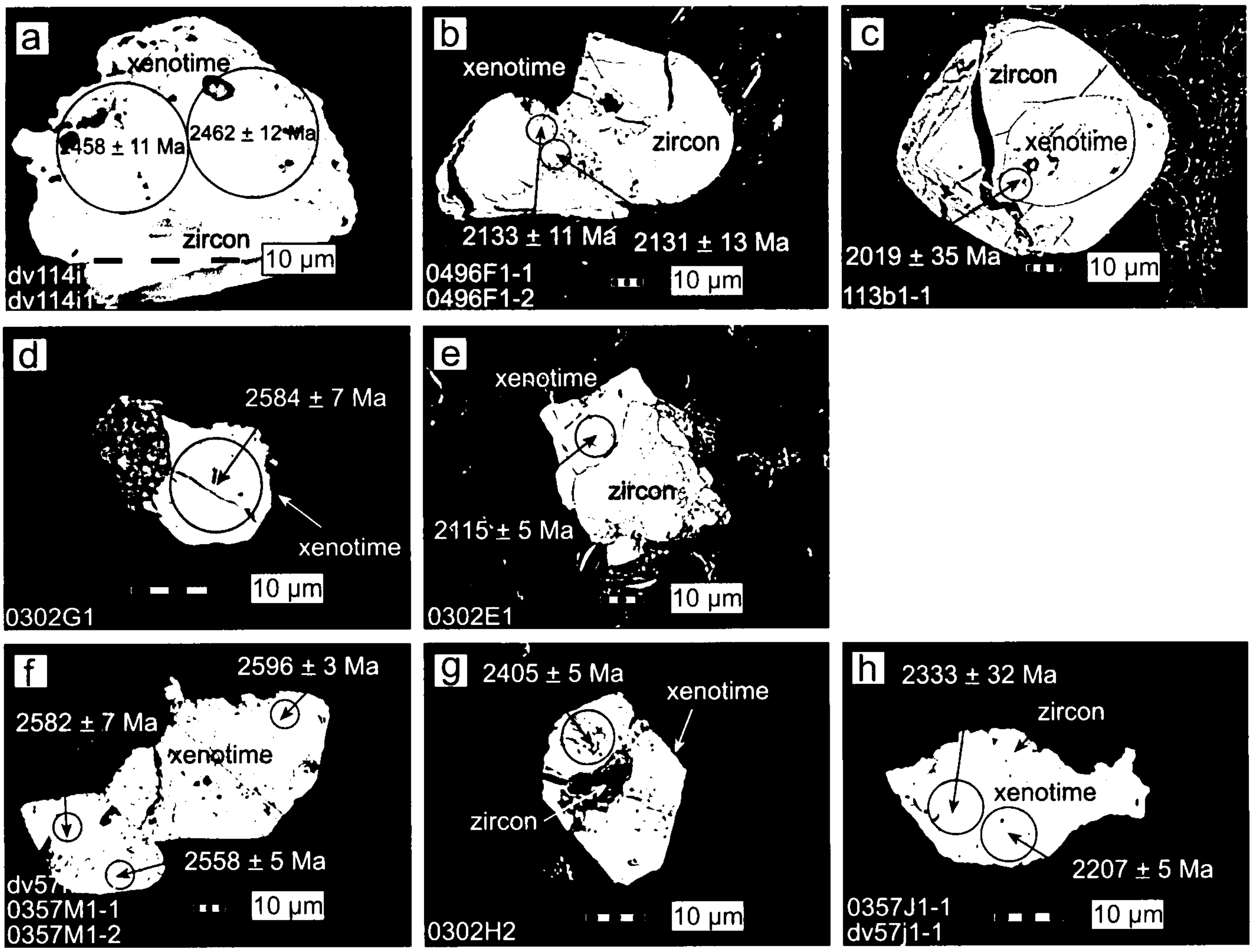

detrital zircon grains from volcanic rocks). It is possible that there were ~2.3 Ga sedimentary–volcanic sequences in Michigan which have mostly been removed, leaving remnants only preserved in the highly altered and deformed (and undated) Dickinson Group and as detrital zircons in the basal units of the Chocolay Group. Recent detrital zircon ages for two samples of the Baraboo Quartzite in southern Wisconsin (Van Wyck and Norman 2004) show a mode at 2.4 Ga with analyses as young as 2.1 Ga. Paleocurrent indicators for the Baraboo Quartzite uniformly show a sediment source to the north (Brett 1955; Dott 1983). There is no evidence in southern Wisconsin for local derivation of these zircon grains, and the authors concluded that either the crustal rocks of this age occur locally and are buried now or the grains record a multicyclic component introduced into the Baraboo Quartzite after long transport distances.

The detrital zircon populations (i.e., 2.7–2.6 Ga, ~2.3 Ga) in the Sturgeon Quartzite and Enchantment Lake Formation are statistically similar; in particular, the ~2.3 Ga detrital zircon populations are within numeric error and may represent the same zircon population. The similarity in the zircon suite from the Enchantment Lake Formation and Sturgeon Quartzite suggests that the sediments shared the same major sources. The Sturgeon Quartzite does not contain the euhedral, needle-like zircon grains as in the Enchantment Lake Formation, yet it contains some ~3 Ga zircon grains (Mississippi Valley terrane?), which suggests that each formation also had minor input from local source areas.

The Archean zircon grains in the Sunday Quartzite (2.7–2.65 Ga) are most likely derived from the Archean greenstone–granite terranes exposed in the Superior craton (Fig. 1). The absence of the ~2.3 Ga detrital zircon population within this data set may reflect its true absence from this formation, or it may be a function of the small (n = 16) sample size being unrepresentative of the sediment sources. Based on a statistical study by Vermeesch (2004), a sample size of 16 means an 80%–85% certainty that no fraction ≥0.2 of the detrital zircon population was missed. However, the predominant well-rounded zircon morphology in the Sunday Quartzite samples, in comparison to the other two formations, suggests that most zircon grains, if not all, came from a different, more distal source. Regardless of interpretation, it can be inferred that the absence or marked reduction in the fraction of ~2.3 Ga zircons within the Sunday Quartzite is a result of the original location of the ~2.3 Ga source(s) in the eastern part of the Animikie Basin. Thus, the deposition of the glaciogenic rocks and most, if not all, of the overlying quartzites with the ~2.3 Ga detrital zircon grains was restricted to the eastern side of the sedimentary basin.

Interpretation of Chocolay Group hydrothermal xenotime ages

The hydrothermal xenotime ages of 2207 ± 5, 2133 ± 11, 2131 ± 13, and 2115 ± 5 Ma in this study are similar to the ages given for some of the 2.2–2.1 Ga dyke swarms emplaced within the Lake Superior Region, particularly the 2121^{+4}_{-7} Ma Marathon dyke swarm (Buchan et al. 1996) in Ontario, north of Lake Superior. It is likely that the hydrothermal xenotime ages record basinal hydrothermal fluid-flow episodes that are associated with the various phases of dyke emplacement during the period of extension within the region, which are related to final breakup of the Kenorland supercontinent (Buchan et al. 1988, 1993, 1996; Roscoe and Card 1993), and that are similar to hydrothermal xenotime growth in metasedimentary rocks because of emplacement of the Bushveld complex (Kositcin et al. 2003). Thus, it can be concluded that the hydrothermal xenotime ages in this study probably record hydrothermal fluid-flow episodes and are not mixtures of ages. Evidence for these thermal episodes also exist in the rocks of the Huronian succession; Nd and Pb isotope data show major metasomatic episodes at about 2.2 Ga (McLennan et al. 2000).

Huronian sedimentation

This study has established that the Chocolay Group in Michigan is correlative with part of the Huronian Supergroup in Ontario—a correlation long-proposed on lithologic similarities, but not previously verified with radiometric age determinations. This now-established correlation allows a firmer reconstruction of the western margin of the Huronian depositional basin. The Chocolay Group is known to extend as far west as the western part of the Gogebic Iron Range in northern Wisconsin (Fig. 1), where a thick (at least 300 m) section of Chocolay Group dolomitic marble is preserved. These outcrops are nearly 500 km west of the westernmost outcrops of the Huronian Supergroup in Ontario, and no doubt these blanket-like carbonate deposits extended considerably farther west than these exposures. If indeed the Chocolay Group is correlated with the Cobalt Group in Ontario, the passive margin phase, which unconformably overlies the early rift phase of the Huronian continental margin, extended far to the west of the classic Huronian area of Ontario. The extent of the basal glaciogenic diamictite is more restricted as it is not known west of the Marquette Iron Range in Michigan, only about 250 km west of the Huronian outcrop belt. The original extent of the glaciogenic diamictite is not clear because of the possibility of a period of erosion between glaciation and the marine transgression marking the base of the overlying quartzites. This study shows that any period of non-deposition was < 100 million years.

It is significant that rocks equivalent to the lower part of the Huronian sequence, the Quirk Lake, Hough Lake, and Elliot Lake groups, are apparently absent in Michigan. This is mirrored in the northeastern part of the Huronian Basin in Ontario where the Cobalt Group lies directly on Archean basement. In much of the Huronian Basin in Ontario, these three groups make up most of the stratigraphic section. They are now generally interpreted to be deposited in rift basins during initial phases of continental breakup (Young et al. 2001, Young 2004), although recent studies (e.g., Barley et al. 2005) relate them to mantle plume breakout events during assembly of the supercontinent.

This study provides evidence for the prior existence of ~2.3 Ga magmatic events in Michigan, of which the Dickinson Group may be a relic. The new evidence presented here, supported by detrital zircon data for the Baraboo Quartzite in southern Wisconsin (Van Wyck and Norman 2004), open a possibility that rifting and sedimentation began in the Michigan area at the same time as that in the Huron Region, but the products of this phase were almost (?) entirely removed before being overlain by the passive margin sequence (i.e., the Chocolay Group). Thus, the base of the Huronian sequence possibly extended much further west then previously considered.

Tectonic evolution

The stratigraphic correlation indicated by our age determinations now allow a more complete sequence of Paleoproterozoic tectonic events to be reconstructed. Because neither the Huronian sequence nor the Marquette Range Supergroup record all of the events it is important to reconstruct a history using both sequences. The early rift phases of the Huronian, only some of which are recognized in the Marquette Range Supergroup as detrital zircon grains (~2.3 Ga) and minor plutons of this age, indicate that rifting began as early as 2.5–2.45 Ga, which is more than 150 million years before deposition of the Chocolay Group in Michigan. On the other hand, the Marquette Range Supergroup records the latter phases of the tectonic cycle, arc accretion, and development of a foreland basin, which occurred more than 325 million years after deposition of the youngest units of the Huronian Supergroup. These events are not recorded in the Huronian Basin, with the possible exception of the locally preserved Whitewater Group of the Huronian which is a likely equivalent of the Baraga Group in Michigan.

Thus, the entire tectonic cycle (or composite of several smaller cycles) from early continental rifts to final ocean closure appears to have spanned more than 600 million years. Of particular interest is the relatively long time interval (up to 325 million years, 2.2–1.875 Ga) between the passive margin sequence (Chocolay Group) and foreland basin sequence (Menominee and Baraga groups) in Michigan. If the culmination of Chocolay Group deposition occurred at ~2.2 Ga as in the Huronian succession, this implies that there was potential for a very large ocean basin to have developed off the southern margin of the Superior craton prior to collision of the first island arc with the continental margin.

Conclusions

This study presents the first geochronological analysis of the Chocolay Group, the basal group of the Marquette Range Supergroup in Michigan. Results indicate:

(1) The basal Enchantment Lake Formation in the Marquette Range contains a detrital zircon population of 2317 ± 6 Ma, with a smaller population at ~2.7 Ga and some zircon analyses at ~2.4 Ga. The stratigraphically higher Sturgeon Quartzite in the Menominee Range contains detrital zircon populations of 2710 ± 6 and 2306 ± 9 Ma, with some analyses around 2.5 and ~3 Ga. The Sunday Quartzite in the Gogebic Range, which is stratigraphically equivalent to the Sturgeon Quartzite, contains a detrital zircon population at 2647 ± 5 Ma but analyses range up to ~2.8 Ga. The Archean detrital zircon grains (i.e., 3.00–2.65 Ma) in each formation are derived from the Archean basement terranes exposed in the Superior craton. The ~2.3 Ga detrital zircon populations in both the Enchantment Lake Formation (Marquette Range) and the Sturgeon Quartzite (Menominee Range) are within numeric error, and they most likely represent a shared ~2.3 Ga source(s). There appears to be an absence, or at least a marked reduction, of the ~2.3 Ga detrital zircon population in the Sunday Quartzite (Gogebic Range), which suggests that the ~2.3 Ga source(s) was located in the eastern part of the basin at the time of Chocolay Group deposition.

(2) There are no known ~2.3 Ga source rocks in the Michigan area. A granite intrusion of ~2.35 Ga has been recorded in Michigan, and ~2.37 Ga granites are recorded in the Lake Huron Region, Ontario. The Dickinson Group in Michigan, which has no radiometric age data and is inferred to be older than the Marquette Range Supergroup, may represent the relic of what were once much more widespread cover sequences in Michigan that have since been mostly removed or concealed. This is supported by detrital zircon ages of ~2.4 Ga in the Baraboo Quartzite in southern Wisconsin, and paleocurrent analysis, which indicates a northerly source direction (Van Wyck and Norman 2004). The Dickinson Group may have been part of the ~2.3 Ga sequence(s) that supplied detrital grains to the eastern parts of the Chocolay Group.

(3) Hydrothermal xenotime ages of 2133 ± 11 and 2131 ± 13 Ma were recorded from the Enchantment Lake Formation, 2115 ± 5 Ma was recorded from a xenotime crystal in the Sturgeon Quartzite, and 2207 ± 5 Ma was recorded from a xenotime crystal in the Sunday Quartzite. These ages are similar to, and probably represent basinal hydrothermal fluid-flow associated with, mafic dyke formation in Minnesota and Ontario that is attributed to the 2.2–2.1 Ga period of extension and magmatism in the Superior craton during the breakup of the Archean (2.8–2.6 Ga) supercontinent referred to as Kenorland.

(4) The maximum depositional age of the Chocolay Group, as well as the base of the Marquette Range Supergroup, is constrained to ~2.3 Ga, and this study interprets the 2.2–2.1 Ga hydrothermal xenotime ages as recording a minimum. This confirms the correlation of the Chocolay Group with part of the Huronian Supergroup.

(5) The evidence for now removed or concealed ~2.3 Ga source rocks, which had to have existed in Michigan prior to Chocolay Group deposition, suggests that rifting and sedimentary deposition may have began in Michigan at about the same time as in the Lake Huron Region.

(6) The unconformity between the Chocolay Group and Menominee Group in Michigan represents a significant gap in time of up to 325 million years, sufficient time for a phase of spreading and development of a very large ocean basin to develop off the southern margin of the Superior craton, prior to the Penokean orogeny.

(7) This study represents a preliminary analysis and should be followed by a more detailed study consisting of larger sample sets of detrital zircons and hydrothermal xenotime.

Acknowledgments

The authors wish to thank Neal J. McNaughton, University of Western Australia, for editorial support in the early stages, and Andrey Bekker, Carnegie Institution of Washington, D.C., Robert M. Easton, Ontario Geological Survey, Ontario, Canada and Richard W. Ojakangas, University of Minnesota Duluth, for supplying some age references. Thanks are also extended to Brendan Griffin and the staff at the Centre for Microscopy and Microanalysis, University of Western Australia, and to Marion Marshall at Minsep Laboratories, University of Western Australia for their individual expertise and technical assistance. The authors wish to thank Drs. B. Davis, Associate Editor, and A. Bekker and K. Sircombe, reviewers, for their time and constructive comments. This work was supported by an Australian Research Council (ARC) grant to N.J. McNaughton and B. Rasmussen. Xenotime analyses were performed at the Western Australian (WA) SHRIMP II facilities, operated by a WA university–government consortium with ARC support. This study is part of a Ph.D. thesis by the first author, undertaken at the University of Western Australia.

References

Allen, R.C., and Barrett, L.P. 1915. A revision of the sequence and structure of the pre-Keweenawan formations of the eastern Gogebic iron range. Michigan Geological and Biological Survey Publication, **18**: 33–83.

Argast, A. 2002. The lower Proterozoic Fern Creek Formation, northern Michigan: mineral and bulk geochemical evidence for its glaciogenic origin. Canadian Journal of Earth Sciences, **39**: 481–492.

Aspler, L.B., and Chiarenzelli, J.R. 1998. Two Neoarchean supercontinents? Evidence from the Paleoproterozoic. Sedimentary Geology, **120**: 75–104.

Barley, M.E., Bekker, A., and Krapez, B. 2005. Late Archean to Early Proterozoic global tectonics, environmental changes and the rise of atmospheric oxygen. Earth and Planetary Science Letters, **238**: 156–171.

Bayley, R.W., Dutton, C.E., and Lamey, C.A. 1966. Geology of the Menominee iron-bearing district Dickinson County, Michigan and Florence and Marinette Counties, Wisconsin. United States Geological Survey, Professional Paper 513.

Brett, G.W. 1955. Cross-bedding in the Baraboo Quartzite, Wisconsin. Journal of Geology, **63**: 143–148.

Buchan, K.L., Card, K.D., and Chandler, F.W. 1988. Multiple ages of Nipissing Diabase intrusions: paleomagnetic evidence from the Englehart area, Ontario. Canadian Journal of Earth Sciences, **26**: 427–445.

Buchan, K.L., Mortensen, J.K., and Card, K.D. 1993. Northeast-trending Early Proterozoic dykes of southern Superior Province: multiple episodes of emplacement recognised from integrated paleomagnetism and U–Pb geochronology. Canadian Journal of Earth Sciences, **30**: 1286–1296.

Buchan, K.L., Halls, H.C., and Mortensen, J.K. 1996. Paleomagnetism, U–Pb geochronology, and geochemistry of Marathon dykes, Superior Province, and comparison with the Fort Frances swarm. Canadian Journal of Earth Sciences, **33**: 1583–1595.

Cannon, W.F., and Gair, J.E. 1970. A revision of stratigraphic nomenclature for middle Precambrian rocks in northern Michigan. Geological Society of America Bulletin, **81**: 2843–2846.

Corfu, F., and Andrews, A. 1986. A U–Pb age for mineralised Nipissing Diabase, Gowganda, Ontario. Canadian Journal of Earth Sciences, **23**: 107–112.

Dawson, G.C., Fletcher, I.R., Krapez, B., McNaughton, N.J., and Rasmussen, B. 2003. 1.2 Ga thermal metamorphism in the Albany–Fraser Orogen of Western Australia: consequence of collision or regional heating by dyke swarms? Journal Geological Society, London, **160**: 29–37.

Dott, R.H.J. 1983. The Proterozoic red quartzite enigma in the north-central US: resolved by plate collision? Geological Society of America, Memoirs 160, pp. 129–141.

Fairbairn, H.W., Hurley, P.M., Card, K.D., and Knight, C.J. 1969. Correlation of radiometric ages of Nipissing Diabase and Huronian metasediments with Proterozoic events in Ontario. Canadian Journal of Earth Sciences, **6**: 489–497.

Fletcher, I.R., Rasmussen, B., and McNaughton, N.J. 2000. SHRIMP U–Pb geochronology of authigenic xenotime and its potential for dating sedimentary basins. Australian Journal of Earth Sciences, **47**: 845–859.

Fletcher, I.R., McNaughton, N.J., Aleinikoff, J.A., Rasmussen, B., and Kamo, S. 2004. Improved procedures and new standards for U–Pb and Th–Pb dating of Phanerozoic xenotime by ion microprobe. Chemical Geology, **209**: 295–314.

Gair, J.E. 1975. Bedrock geology and ore deposits of the Palmer Quadrangle, Marquette County, Michigan. United States Geological Survey, Professional Paper 769, p. 159.

Gair, J.E. 1981. Lower Proterozoic glacial deposits of northern Michigan, USA. *In* Earth's pre-Pleistocene glacial record. *Edited by* M.J. Hambrey and W.B. Harland. Cambridge University Press, Cambridge, UK, pp. 803–806.

Gair, J.E., and Thaden, R.E. 1968. Geology of the Marquette and Sands Quadrangles, Marquette County, Michigan. United States Geological Survey, Professional Paper 397, p. 77.

Graff, P. 1979. A review of the stratigraphy and uranium potential of Early Proterozoic (Precambrian X) metasediments in the Sierra Madre, Wyoming. University of Wyoming Contributions to Geology, **17**: 149–157.

Hammond, R.D. 1978. Geochronology and origin of Archean rocks in Marquette County, Michigan. M.Sc. thesis, University of Kansas, Lawrence, Kansas.

Heaman, L.M. 1997. Global mafic magmatism at 2.45 Ga: remnants of an ancient large igneous province? Geology, **25**: 299–302.

Hoffman, P.F. 1992. Supercontinents. *In* Encyclopedia of earth system science. Vol. 4. Academic Press, London, UK, pp. 323–328.

Houston, R.S., Lanthier, L.R., Karlstrom, K.E., and Sylvester, G. 1981. Early Proterozoic diamictite of southern Wyoming. *In* Earth's pre-Pleistocene glacial record. *Edited by* M.J. Hambrey and W.B. Harland. Cambridge University Press, Cambridge, UK, pp. 795–799.

James, H.L. 1955. Zones of regional metamorphism in the Precambrian of northern Michigan. Geological Society of America Bulletin, **67**: 1455–1488.

James, H.L. 1958. Stratigraphy of pre-Keweenawan rocks in parts of northern Michigan. United States Geological Survey Professional Paper 314-C, pp. 27–41.

James, H.L., Clark, L.D., Lamey, C.A., and Pettijohn, F.J. 1961. Geology of central Dickinson County, Michigan. United States Geological Survey, Professional Paper 310, p. 176.

Kositcin, N., McNaughton, N.J., Griffin, B.J., Fletcher, I.R., Groves, D.I., and Rasmussen, B. 2003. Textural and geochemical discrimination between xenotime of different origin in the Archaean Witwatersrand Basin, South Africa. Geochimica et Cosmochimica Acta, **67**: 709–731.

Krogh, T.E., Davis, D.W., and Corfu, F. 1984. Precise U–Pb zircon and baddeleyiteages for the Sudbury area. *In* The geology and ore deposits of the Sudbury Structure. *Edited by* G.E. Pye, A.J. Naldrett and P.E. Giblin. Ontario Geological Survey, Special Paper 1, pp. 449–489.

Krogh, T.E., Kamo, S.E., and Bohor, B.F. 1996. Shock metamorphosed zircons with correlated U–Pb discordance and melt rocks with concordant protolith ages indicate an impact origin for the Sudbury structure. Amercian Geophysical Union, Monograph 95, pp. 343–353.

Larue, D.K. 1981. The Chocolay Group, Lake Superior Region, USA: Sedimentologic evidence for deposition in basinal and platform settings on an early Proterozoic craton. Geological Society of America Bulletin, **92**: 417–435.

Larue, D.K., and Sloss, L.L. 1980. Early Proterozoic sedimentary basins of the Lake Superior Region. Geological Society of America Bulletin, **91**: 450–452.

Long, D.F. 1981. Glacigenic rocks in the Early Proterozoic Chibougamau Formation of northern Quebec. *In* Earth's pre-Pleistocene glacial record. *Edited by* M.J. Hambrey and W.B. Harland. Cambridge University Press, Cambridge, UK, pp. 817–820.

Ludwig, K.R. 2001. Isoplot/Ex: a geochronological toolkit for Microsoft Excel. Berkeley Geochronology Center, Special Publication 1a, pp. 56.

McLennan, S.M., Simonetti, A., and Goldstein, S.L. 2000. Nd and Pb isotopic evidence for provenance and post-depositional alteration of the Paleoproterozoic Huronian Supergroup, Canada. Precambrian Research, **102**: 263–278.

McNaughton, N.J., Rasmussen, B., and Fletcher, I.R. 1999. SHRIMP uranium–lead dating of diagenetic xenotime in siliciclastic sedimentary rocks. Science, **285**: 78–80.

Nelson, D.R. 1997. Compilation of SHRIMP U–Pb zircon geochronology data, 1996. Western Australian Geological Survey Record 1997/2.

Ojakangas, R.W. 1982. Lower Proterozoic glaciogenic formations, Marquette Supergroup, Upper Peninsula, Michigan, USA. International Association of Sedimentologists International Congress on Sediment, Abstract 11, p.76.

Ojakangas, R.W. 1985. Evidence for early Proterozoic glaciation: the dropstone unit–diamictite association. Geological Survey Finland Bulletin, **331**: 55–72.

Ojakangas, R.W. 1988. Glaciation: an uncommon mega-event as a key tointracontinental and intercontinental correlation of Early Proterozoic basin fill, North American and Baltic cratons. *In* New perspectives in basin analysis. *Edited by* K.L. Kleinspehn and C. Paola. Springer, Berlin, Germany, pp. 431–444.

Ojakangas, R.W., Morey, G.B., and Southwick, D.L. 2001. Paleoproterozoic basin development and sedimentation in the Lake Superior Region, North America. Sedimentary Geology, **141–142**: 319–341.

Pettijohn, F.J. 1943. Basal Huronian conglomerates of Menominee and Calumet districts, Michigan. Journal of Geology, **51**: 387–397.

Puffett, W.P. 1969. The Reany Creek Formation, Marquette County, Michigan. United States Geological Survey Bulletin, **1274**: 25.

Rasmussen, B. 1996. Early diagenetic REE–phosphate minerals (florencite, gorceixite, crandellite, and xenotime) in marine sandstones: a major sink for oceanic phosphorus. American Journal of Science, **296**: 601–632.

Rasmussen, B., and Fletcher, I.R. 2002. Indirect dating of mafic intrusions by SHRIMP U–Pb analysis of monazite in contact metamorphosed shale: an example from the Capricorn Orogen, Western Australia. Earth and Planetary Science Letters, **197**: 287–299.

Rasmussen, B., Fletcher, I.R., and McNaughton, N.J. 2001. Dating low-grade metamorphic events by SHRIMP U–Pb analysis of monazite in shales. Geology, **29**: 963–966.

Rasmussen, B., Bengtson, S., Fletcher, I.R., and McNaughton, N.J. 2002. Discoidal impressions and trace-like fossils more than 1200 million years old. Science, **292**: 1112–1115.

Rasmussen, B., Fletcher, I.R., Bengtson, S., and McNaughton, N.J. 2004. SHRIMP U–Pb dating of diagenetic xenotime in the Stirling Range Formation, Western Australia:1.8 billion year minimum age for the Stirling biota. Precambrian Research, **133**: 329–337.

Romano, D., Holm, D., and Foland, K. 2000. Determining the extent and nature of Mazatzal-related overprinting of the Penokean orogenic belt in the southern Lake Superior Region, north-central USA. Precambrian Research, **104**: 25–46.

Roscoe, S.M., and Card, K.D. 1993. The reappearance of the Huronian in Wyoming: rifting and drifting of ancient continents. Canadian Journal of Earth Sciences, **30**: 2475–2480.

Schneider, D., Holm, D., and Lux, D. 1996. On the origin of Early Proterozoic gneiss domes and metamorphic nodes, northern Michigan. Canadian Journal of Earth Sciences, **33**: 1053–1063.

Schneider, D.A., Bickford, M.E., Cannon, W.F., Schulz, K.J., and Hamilton, M.A. 2002. Age of volcanic rocks and syndepositional iron formation, Marquette Range Supergroup: implications for the tectonic setting of Paleoproterozoic iron formation of the Lake Superior Region. Canadian Journal of Earth Sciences, **39**: 999–1012.

Schneider, D.A., Holm, D.K., O'Boyle, C.O., Hamilton, M., and Jercinovic, M. 2004. Paleoproterozoic development of a gneiss dome corridor in the southern Lake Superior Region, USA. *In* Gneiss domes in orogeny. *Edited by* D.L. Whitney and C.S. Siddoway. Geological Society of America, Special Paper 380. pp. 339–357.

Sims, P.K., Van Schmus, W.R., Schulz, K.J., and Peterman, Z.E. 1989. Tectonostratigraphic evolution of the Early Proterozoic Wisconsin magmatic terranes of the Penokean orogen. Canadian Journal of Earth Sciences, **26**: 2145–2158.

Smith, M.D. 2002. The timing and petrogenesis of the Creighton pluton, Ontario: an example of felsic magmatism associated with Matachewan igneous events. M.Sc. thesis, The University of Alberta, Edmonton, Alta.

Smith, J.B., Barley, M.E., Groves, D.I., Krapez, B., McNaughton, N.J., Bickle, M.J., and Chapman, H.J. 1998. The Scholl Shear Zone, West Pilbara: evidence for a domain boundary structure from integrated tectonostratigraphic analyses, SHRIMP U–Pb dating and isotopic and geochemical data of granitoids. Precambrian Research, **88**: 143–171.

Southwick, D.L., and Day, W.C. 1983. Geology and petrology of Proterozoic mafic dikes, north-central Minnesota and western Ontario. Canadian Journal of Earth Sciences, **20**: 622–638.

Taylor, G.L. 1972. Stratigraphy, sedimentology and sulphide mineralisation of the Kona Dolomite. PhD thesis, Michigan Technological Institute, Lansing, Mich.

Tinkham, D.K., and Marshak, S. 2004. Precambrian dome and keel structures in the Penokean orogenic belt of northern Michigan, USA. *In* Gneiss domes in orogeny. *Edited by* D.L. Whitney and C.S. Siddoway. Geological Society of America, Special Paper 380, pp. 321–338.

United States Geological Survey. 1982. Topographic map of Escanaba, Michigan–Wisconsin, Map 45087-E1-TM-100, series 30′ × 60′, scale 1 : 100 000.

United States Geological Survey. 1985. Topographic map of Marquette, Michigan. Map 46087-E1-TM-100, series 30′ × 60′, scale 1 : 100 000.

United States Geological Survey. 1990. Topographic map of Wakefield, Michigan–Wisconsin. Map 46089-A1-TM-100, series 30′ × 60′, scale 1 : 100 000.

Vallini, D., Rasmussen, B., Krapez, B., Fletcher, I.R., and McNaughton, N.J. 2002. Obtaining diagenetic ages from metamorphosed sedimentary rocks: U–Pb dating of unusually coarse xenotime cement in phosphatic sandstone. Geology, **30**: 1083–1086.

Vallini, D., Rasmussen, B., Krapez, B., Fletcher, I.R., and McNaughton, N.J. 2005. Microtextures, geochemistry and geochronology of authigenic xenotime: constraining the cementation history of a Palaeoproterozoic metasedimentary sequence. Sedimentology, **52**: 101–122.

Vallini, D., Groves, D.I., McNaughton, N.J., and Fletcher, I.R. In press. Uraniferous diagenetic xenotime in northern Australia and its relationship to unconformity-associated uranium mineralisation. Mineralium Deposita.

Van Schmus, W.R. 1965. The geochronology of the Bruce Mines – Blind River area, Ontario, Canada. Journal of Geology, **73**: 755–780.

Van Schmus, W.R. 1976. Early and Middle Proterozoic history of the Great Lakes area, North America. Royal Society of London Philosophical Transactions, Series A, **280**: 605–628.

Van Wyck, N., and Norman, N. 2004. Detrital zircon ages from Early Proterozoic quartzite, Wisconsin, support rapid weathering and deposition of mature quartz arenites. The Journal of Geology, **112**: 305–315.

Vermeesch, P. 2004. How many grains are needed for a provenance study? Earth and Planetary Science Letters, **224**: 441–451.

Vielreicher, N.M., Groves, D.I., Fletcher, I.R., McNaughton, N.J., and Rasmussen, B. 2003. Hydrothermal monazite and xenotime geochronology: a new direction for precise dating of orogenic gold mineralization. Society of Economic Geology Newsletter, **53**: 10–16.

Williams, H., Hoffman, P.F., Lewry, J.F., Monger, J.W.H., and Rivers, T. 1991. Anatomy of North America: thematicgeologic portrayals of the continent. Tectonophysics, **187**: 117–134.

Wirth, K.R., Vervoort, J.D., and Heaman, L.M. 1995. Nd isotopic constraints or mantle and crustal contributions to 2.08 Ga diabase dykes of the southern Superior province. Annual International Dyke Conference, Jerusalem, Israel. Program and Abstracts, Abstract 3, p. 64.

Young, G.M. 1970. An extensive Early Proterozoic glaciation in North America? Palaeogeographical, Palaeoclimatol, Palaeoecological, **7**: 85–101.

Young, G.M. 1973. Tillites and aluminous quartzites as possible time markers for middle Precambrian (Aphebian) rocks of North America. Geological Association of Canada, Special Paper 12, pp. 97–127.

Young, G.M. 1983. Tectono–sedimentary history of early Proterozoic rocks of the northern Great Lakes Region. *In* Early Proterozoic geology of the Great Lakes Region. *Edited by* L.G. Jr. Medaris. Geological Society America, Memoir 160, pp.15–32.

Young, G.M. 1991. Stratigraphy, sedimentology and tectonic setting of the Huronian Supergroup. *In* Geological Association of Canada – Society of Economic Geology, Joint Annual Meeting. Fieldtrip Guidebook B5.

Young, G. M. 2004. Earth's earliest extensive glaciations: tectonic setting and stratigraphic context of Paleoproterozoic glaciogenic deposits. *In* The extreme Proterozoic: geology, geochemistry, and climate. American Geophysical Union, Geophysical Monograph Series 146, pp. 161–181.

Young, G.M., and McClennan, S.M. 1981. Early Proterozoic Padlei Formation, Northwest Territories, Canada. *In* Earth's pre-Pleistocene glacial record. *Edited by* M.J. Hambrey and W.B. Harland. Cambridge University Press, Cambridge, UK, pp. 790–794.

Young, G.M., Long, D.G.F., Fedo, C.M., and Nesbitt, H.W. 2001. PaleoproterozoicHuronian basin: product of a Wilson cycle punctuated by glaciations and a meteoriteimpact. Sedimentary Geology, **141–142**: 233–254.